

**Computational Fragment-based Discovery of Allosteric Modulators on Metabotropic  
Glutamate Receptor 5**

by

**Yuemin Bian**

Bachelor's degree, China Pharmaceutical University, 2015

Submitted to the Graduate Faculty of  
School of Pharmacy in partial fulfillment  
of the requirements for the degree of  
Master of Science

University of Pittsburgh

2017

UNIVERSITY OF PITTSBURGH

SCHOOL OF PHARMACY

This thesis was presented

by

Yuemin Bian

It was defended on

March 30<sup>th</sup>, 2017

and approved by

Lee McDermott, PhD, Assistant Professor, Department of Pharmaceutical Science

Xiang-Qun (Sean) Xie, PhD, EMBA, Professor, Department of Pharmaceutical Science

Peng Yang, PhD, Assistant Professor, Department of Pharmaceutical Science

Thesis Director: Xiang-Qun (Sean) Xie, PhD, MD, EMBA, Department of Pharmaceutical

Science

Copyright © by Yuemin Bian

2017

# Computational Fragment-based Discovery of Allosteric Modulators on Metabotropic Glutamate Receptor 5

Yuemin Bian, B.S.

University of Pittsburgh, 2017

## ABSTRACT

GPCR allosteric modulators target at the allosteric, “*allo-* from the Greek meaning “other”, binding pockets of G protein-coupled receptors (GPCRs) with indirect influence on the effects of an agonist or inverse agonist. Such modulators exhibit significant advantages compared to the corresponding orthosteric ligands, including better chemical tractability or physicochemical properties, improved selectivity, and reduced risk of over-sensitization towards their receptors. Metabotropic glutamate receptor 5 (mGlu<sub>5</sub>), a member of GPCRs class C family, is a promising therapeutic target for treating many central nervous system (CNS) diseases. The crystal structure of mGlu<sub>5</sub> in the complex with the negative allosteric modulator (NAM) mavoglurant was recently reported, providing a fundamental model for the design of new allosteric modulators. However, new NAM drugs are still in critical need for therapeutic uses. Computational fragment-based drug discovery (FBDD) represents a powerful scaffold-hopping and lead structure-optimization tool for drug design. In the present work, a set of integrated computational methodologies was first used, such as fragment library generation and retrosynthetic combinatorial analysis procedure (RECAP) for novel compound generation. Then, the new compounds generated were assessed by benchmark dataset verification, docking studies, and QSAR model simulation. Subsequently, the structurally

diverse compounds, with reported or unreported scaffolds, can be observed from the top 20 *in silico* design/synthesized compounds, which were predicted to be potential mGlu<sub>5</sub> allosteric modulators. The *in silico* designed compounds with reported scaffolds may fill SAR holes in the known, patented series of mGlu<sub>5</sub> modulators. And the generation of compounds without reported activities on mGluR indicates that our approach is doable for exploring and designing novel compounds. Our case study of designing allosteric modulators on mGlu<sub>5</sub> demonstrated that the established computational fragment-based approach is a useful methodology for facilitating new compound design and synthesis in the future.

**Keywords:** Allosteric modulator, Computational fragment-based drug discovery, Metabotropic glutamate receptor 5, GPCRs

## TABLE OF CONTENTS

<b>PREFACE.....</b>	<b>xi</b>
<b>1.0 INTRODUCTION.....</b>	<b>1</b>
<b>1.1 ORTHOSTERIC AND ALLOSTERIC REGULATIONS OF GPCRS .....</b>	<b>1</b>
<b>1.2 GLUTAMATE RECEPTORS.....</b>	<b>6</b>
<b>1.3 FRAGMENT-BASED DRUG DESIGN .....</b>	<b>8</b>
<b>2.0 MATERIALS AND METHODS .....</b>	<b>12</b>
<b>2.1 X-RAY STRUCTURES AND GPCR ALLOSTERIC MODULATORS .....</b>	<b>12</b>
<b>2.2 FRAGMENTS GENERATION AND <i>IN SILICO</i> SYNTHESIS.....</b>	<b>13</b>
<b>2.3 MOLECULAR DOCKING FOR THE STUDIES OF mGlu<sub>5</sub>-LIGANDS</b> <b>INTERACTION.....</b>	<b>13</b>
<b>2.4 GENERATION OF BENCHMARKING DATASET .....</b>	<b>14</b>
<b>2.5 QUANTITATIVE STRUCTURE-ACTIVITY RELATIONSHIP MODEL .....</b>	<b>15</b>
<b>3.0 RESULTS .....</b>	<b>15</b>
<b>3.1 STUDY DESIGN AND THE STRATEGIES FOR DESIGNING NOVEL</b> <b>COMPOUNDS .....</b>	<b>16</b>
<b>3.2 THE ESTABLISHMENT OF FRAGMENT LIBRARY .....</b>	<b>17</b>
<b>3.3 DOCKING STUDIES OF FRAGMENTS INTO mGlu<sub>5</sub> .....</b>	<b>19</b>
<b>3.4 <i>IN SILICO</i> SYNTHESIS OF NOVEL COMPOUNDS FROM CATEGORIZED</b> <b>FRAGMENTS.....</b>	<b>22</b>
<b>3.5 ENRICHMENT TEST WITH A BENCHMARKING DATASET.....</b>	<b>28</b>
<b>3.6 PREDICTION OF COMPETITION BINDING WITH A QSAR MODEL.....</b>	<b>29</b>

<b>3.7 VALIDATION WITH PAINS-REMOVER AND TOXTREE.....</b>	<b>32</b>
<b>3.8 THE EFFECTS ON LIGANDS AND FRAGMENTS BINDING CAUSED BY THE ROTATION OF TRP785 .....</b>	<b>33</b>
<b>4.0 DISCUSSION .....</b>	<b>36</b>
<b>5.0 CONCLUSION .....</b>	<b>41</b>
<b>6.0 FUTURE PROSPECTIVE.....</b>	<b>42</b>
<b>6.1 METABOTROPIC GLUTAMATE RECEPTOR 5 ALLOSTERIC REGULATION .....</b>	<b>42</b>
<b>6.2 CANNABINOID RECEPTOR 2 ALLOSTERIC REGULATION.....</b>	<b>43</b>
<b>7.0 APPENDIX.....</b>	<b>44</b>
<b>7.1 120 HIGHEST SCORED FRAGMENTS IN THE UPPER REGION .....</b>	<b>44</b>
<b>7.2 80 HIGHEST SCORED FRAGMENT IN THE BOTTOM REGION.....</b>	<b>53</b>
<b>7.3 124 <i>IN SILICO</i> SYNTHESIZED COMPOUNDS WITH DOCKING SCORE OVER 7 .....</b>	<b>58</b>
<b>7.4 DECOYS INVOLVED IN THE ENRICHMENT TEST .....</b>	<b>71</b>
<b>7.5 <i>KI</i> VALUE AND PHYSICAL PROPERTIES OF 66 1,2-DIPHENYLETHYNE ANALOGS.....</b>	<b>76</b>
<b>7.6 ABBREVIATIONS.....</b>	<b>82</b>
<b>8.0 BIBLIOGRAPHY .....</b>	<b>84</b>

## LIST OF FIGURES

FIGURE 1. The number of publications each year including the concept of “allosteric modulator” .....	2
FIGURE 2. Categorization of GPCRs’ orthosteric ligands and allosteric modulators .....	3
FIGURE 3. Crystallized structure of mGlu5 transmembrane domain in complex with mavoglurant .....	7
FIGURE 4. Commonly used strategies for fragment-based drug design .....	9
FIGURE 5. Flowchart of computational fragment-based drug design .....	11
FIGURE 6. Study design and strategies for designing novel mGlu5 allosteric modulators.	17
FIGURE 7. Allosteric binding site of mGlu <sub>5</sub> .....	20
FIGURE 8. Fragment docking studies .....	21
FIGURE 9. Fragments sorting .....	22
FIGURE 10. Distribution of the docking scores for small scale RECAP Synthesis .....	23
FIGURE 11. Correlation plot for docking score and binding energy .....	27
FIGURE 12. In silico synthesis of potential mGlu5 allosteric modulators .....	28
FIGURE 13. The enrichment test with decoys .....	29
FIGURE 14. Correlation plot for quantitative structure-activity relationship model .....	32
FIGURE 15. Assessment on the rotation of Trp785 .....	35
FIGURE 16. Fragments sorting based on 5CGD .....	36



FIGURE 17. Structural comparison between in silico synthesized compounds and existing compounds with known mGluR allosteric activities. ....	39
--	----

## LIST OF TABLES

TABLE 1. Allosteric modulators and bitopic ligands with a status of marketed or under clinical evaluation.....	4
TABLE 2. Structure and properties for top ten most frequently appeared fragments .....	18
TABLE 3. Docking score, binding energy and predicted Ki value for top 20 in silico synthesized compounds. ....	24
TABLE 4. Descriptors of linear regression analysis .....	30
SUPPLEMENTARY TABLE 1. 120 highest scored fragments in the upper region .....	44
SUPPLEMENTARY TABLE 2. 80 highest scored fragments in the bottom region .....	53
SUPPLEMENTARY TABLE 3. 124 <i>in silico</i> synthesized compounds with docking score over 7 .....	59
SUPPLEMENTARY TABLE 4. Properties of mavoglurant and benchmarking decoys .....	71
SUPPLEMENTARY TABLE 5. <i>Ki</i> value and physical properties of 66 1,2-diphenylethyne analogs .....	76

## PREFACE

I can never forget the first time when I met with Dr. Qiang-Qun Xie, my advisor, during my first day in University of Pittsburgh. He gave me a warm welcome to join the group and to continue my graduate education. Instead of directly talking about his requirements and laboratory policies, Dr. Xie raised one inspiring question, “*What is the motivation for you to participating in the area of scientific research?*” There are more than one hundred reasons that one person should not participate, but the strongest interest towards the field of Pharmaceutical Science driven me here. During the two years of work, I kept asking myself this question. Have I lost my motivation? Have I kept my interest in this field? Since my strongest interest is always there, I keep learning, keep thinking, and keep improving myself. Thank you Dr. Xie not only for your wholehearted guidance and support, but also for your inspirations to help me overcome the obstacles in my research work.

Also, I would like to express my gratefulness to Dr. Zhiwei Feng. As an expert in the field of Computational-Aided Drug Design, Dr. Feng is experienced and knowledgeable. Any time when I faced with a problem, Dr. Feng would provide constructive recommendations. As I was developing my study design, I always enjoyed the discussion with Dr. Feng, because of his valuable comments and critical suggestions.

Meanwhile, I would like to thank Dr. Peng Yang, and Dr. Lirong Wang. As an experienced Medicinal Chemist and my group leader, Dr. Yang shared his experiences of diversified compounds design with me. And I always remember that it is Dr. Yang, who carefully revised my seminar slides and polished it up. Dr. Wang is a sophisticated scientist in the field of

Pharmacogenomics. Dr. Wang let me participated in multiple projects, which enabled me to practice more and broaden my scope.

At the same time, let me express my sincere acknowledgement to all the members in Dr. Xiang-Qun Xie's group. I enjoy each discussion with group members. I enjoy each suggestion and comment proposed during our group meeting. And, I enjoy the every minute I spent with all of you.

At last, I would like to mention my parents. Definitely, the words "thank you" are far less enough to express my emotion in this very moment. Sorry for the superficial study on building up my vocabulary.

锦书托何处？离索几春秋。应怜莫江水，不作一处流。

There is no word that can express one per cent, if not point one per cent, of my gratefulness and miss to my dear parents.

I offer my warmest regards and sincere blessings to all of those who helped me during the completion of this project in any respect.

## 1.0 INTRODUCTION

### 1.1 ORTHOSTERIC AND ALLOSTERIC REGULATIONS OF GPCRS

The human G protein-coupled receptors (GPCRs), which can also be described as 7-transmembrane (TM) receptors account for more than 1% of human genome. The GPCR superfamily, comprised more than 800 receptors, can be further categorized into four different classes, class A, B, C, and F (Frizzled), according to their sequence homology.(1, 2) As essential receptors associated with a variety of physiological processes, including neurotransmission, immune defense, and cell growth, over 30% of currently marketed drugs are using GPCRs as their targets.(3, 4)

Each GPCR possesses an orthosteric binding pocket for its respective endogenous ligands. Compounds derived from nature sources or chemical synthesis binding to this pocket are termed orthosteric ligands.(5) Early drug development was focused on the orthosteric modulation and almost all of the FDA-approved compounds for therapeutic use target at the orthosteric binding sites of the receptors.(5, 6) However, the ligands coming out from this strategy have drawbacks including limited or poor selectivity, a lack of efficacy, and resistance or decreased efficacy upon chronic administration.(7-9) GPCRs can have allosteric binding sites, which have topological and functional distinctions from corresponding orthosteric binding sites. The existence of allosteric binding pockets allows additional interactions between ligands and receptors. And the benzodiazepine class of compounds is a prime example of successful allosteric modulators.(5, 10, 11) As shown in **Figure 1**, the number of publications that include the concept of “allosteric

modulators” per year has been increased, and the trend continues. Notably, more than 450 papers were published in 2016, which illustrates the elevated interests of allosteric regulation.

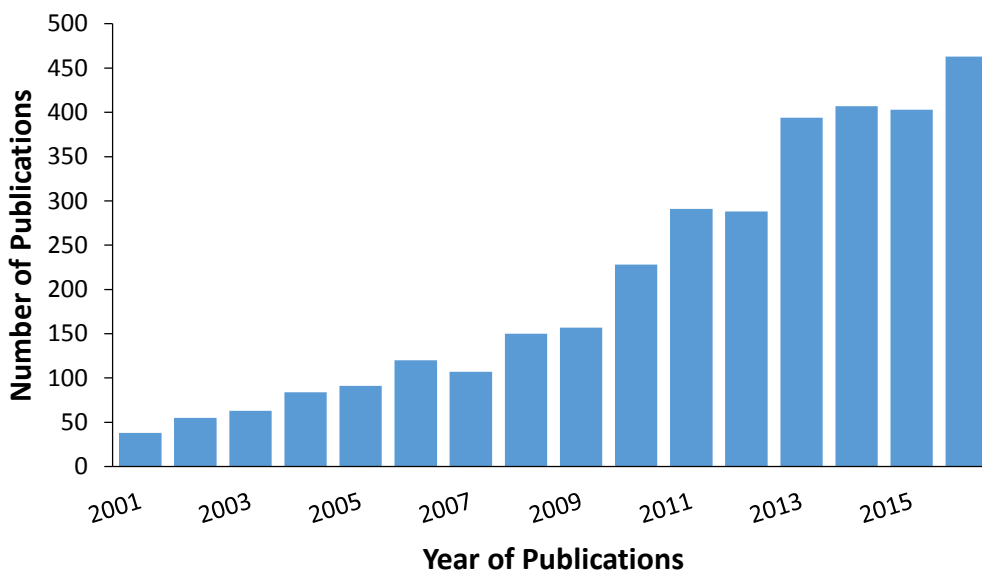


**Figure 1.** The number of publications each year including the concept of “allosteric modulator”

The search of papers on SciFinder with the key words “allosteric modulator” from 2001 to 2016 demonstrate a trend of increased publications.

Across a receptor family, the allosteric pockets usually stand with less evolutionary pressure for conservation, and the corresponding allosteric ligands usually have better selectivity. Meanwhile, allosteric ligands have a ceiling effect, which means their effects are saturable.(12, 13) Usually, orthosteric ligands could be categorized into agonist, antagonist, partial agonist, and inverse agonist, according to the physiological responses they trigger (**Figure 2A**). Based on the modes of pharmacology, allosteric ligands can be categorized into positive allosteric modulators (PAMs), which enhance agonist-mediated receptor response, negative allosteric modulators (NAMs), which noncompetitively attenuate orthosteric activities, and silent allosteric modulators

(SAMs), which have no effect on responses triggered by orthosteric ligands but block the effects caused by PAMs and NAMs (**Figure 2B**).<sup>(5)</sup>

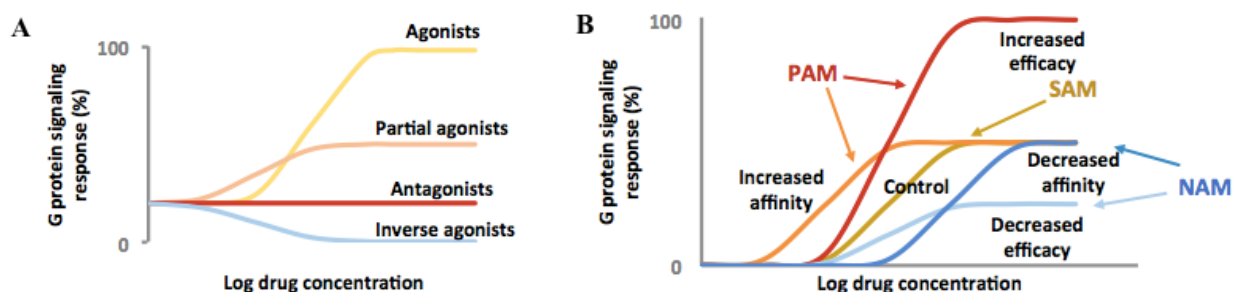


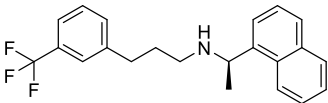
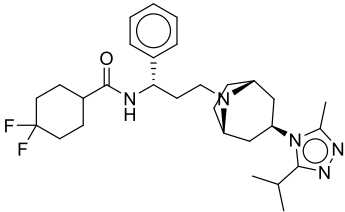
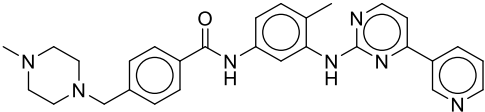
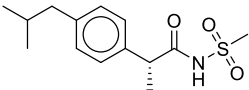
**Figure 2.** Categorization of GPCRs' orthosteric ligands and allosteric modulators

**A.** The categorization of orthosteric ligands. An agonist is a ligand that could bind the receptor and fully activate the receptor to produce a biological response. A partial agonist is a ligand that could also bind the receptor, but only partially activate the receptor. An antagonist is a ligand that could bind and block the receptor and prevent the generation of biological response. An inverse agonist is a ligand that binds the same receptor as an agonist but triggers opposite biological response. **B.** The categorization of allosteric modulators. Allosteric modulators occupy allosteric binding pocket. A positive allosteric modulator (PAM) could increase the affinity or efficacy of the orthosteric agonist. A negative allosteric modulator (NAM) could decrease the affinity or efficacy of the orthosteric ligand. A silent allosteric modulator could only occupy the binding pocket, but does not have any influence on orthosteric ligands.

The clinical success of the benzodiazepines suggests that allosteric regulation is a promising therapeutic strategy.<sup>(14)</sup> Cinacalcet and Maraviroc are two famous examples of successful developments of allosteric modulators. Cinacalcet is a positive allosteric modulator for calcium-sensing receptor, and got approved by FDA in March 2004. Maraviroc is a negative

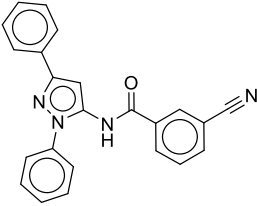
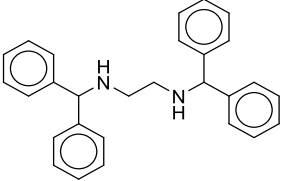
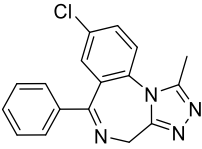
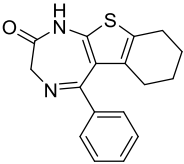
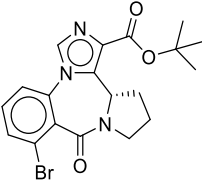
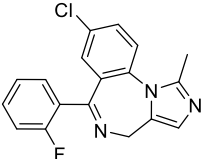
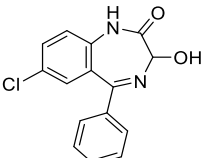
allosteric modulator for CCR5 used in the treatment of HIV infection to prevent the fusion of the virus and the T cells. The Maraviroc was approved by FDA in August 2007. Meanwhile, a new category of ligands, termed bitopic ligands, emerged. Bitopic ligands should target the orthosteric binding pocket and allosteric binding pocket simultaneously. Giving that orthosteric ligands usually have the high affinity towards the receptor, and allosteric ligands would have better selectivity, designing bitopic ligands has the potential to combine these advantages. Tahtaoui and his group synthesized a series derivatives for M1AChR antagonist in 2004. The receptor-ligand interactions were assessed, and the authors found that these analogs could have interactions with both the orthosteric binding site and the allosteric binding site of the receptor. Therefore, these derivatives behave as potential bitopic ligands. **Table 1** shows the currently marketed drugs and compounds in clinical trials that function as allosteric or bitopic ligands.

**Table 1.** Marketed or under clinical investigation allosteric and bitopic ligands

No.	Drug	Structure	Target	Indication and Stages
1	Cinacalcet (PAM)		CaSR	FDA-approved for Hyperparathyroidism
2	Maraviroc (NAM)		CCR5	FDA-approved for HIV
3	Imatinib (NAM)		BCR/ABL and KIT	FDA-approved for chronic myelogenous leukemia
4	Reparixin (NAM)		CXCR1/CXCR2	Phase II/III for reperfusion injury to lung/kidney transplantation



5	MK2206 (NAM)		AKT1, AKT2, AKT3	Phase II for acute lymphoblastic leukemia
6	AZD2423 (NAM)		CCR2	Phase II for neuropathic pain
7	Norclozapine (PAM)		ACM1	Phase II Schizophrenia
8	Litronesib (NAM)		KNSL1	Phase II antineoplastic activity
9	ADX71149 (PAM)		mGluR2	phase II for schizophrenia
10	AZD8529 (PAM)		mGluR3/2	phase II for schizophrenia
11	STX107 (NAM)	--	mGluR5	Phase III for Fragile X, Phase II for autism
12	AFQ056 (NAM)		mGluR5	Phase II completed PD-LID, Fragile X
13	Dipraglurant (NAM)		mGluR5	Phase II PD-LID, Dystonia
14	RO 4917523 (NAM)		mGluR5	Phase II for Fragile X, depression
15	Fenobam (NAM)		mGluR5	Phase II for Fragile X

16	CDPPB (PAM)		mGluR5	depression
17	AMN082 (PAM)		mGluR7	Phase II for hypercholesterolemi a
18	Alprazolam (PAM)		GABAA	anxiolytic
19	Benzazepam (PAM)		GABAA	anxiolytic
20	Bretazenil (PAM)		GABAA	anxiolytic, anticonvul sant
21	Midazolam		GABAA	hypnotic, anticonvulsant
22	Oxazepam		GABAA	anxiolytic

## 1.2 GLUTAMATE RECEPTORS

Metabotropic glutamate receptor 5 (mGlu5) is a member of class C GPCRs, which mainly responds to glutamate, one of the major neurotransmitters.(15) Class C GPCRs include

metabotropic glutamate receptors, taste receptors, calcium-sensing receptors, GABA<sub>B</sub> and others. mGlu<sub>5</sub> is a promising drug target for the treatment of diseases ranging from fragile X syndrome to depression and movement disorders.(16) mGlu<sub>5</sub> negative allosteric modulators, which could attenuate orthosteric ligands mediated mGlu<sub>5</sub> activation, are under clinical evaluation for the treatment of multiple diseases.(17, 18) Dr. Fiona H. Marshall and her group have reported the crystal structure of the transmembrane domain of human mGlu<sub>5</sub> receptor, in the complex with the negative allosteric modulator mavoglurant (Figure 3).

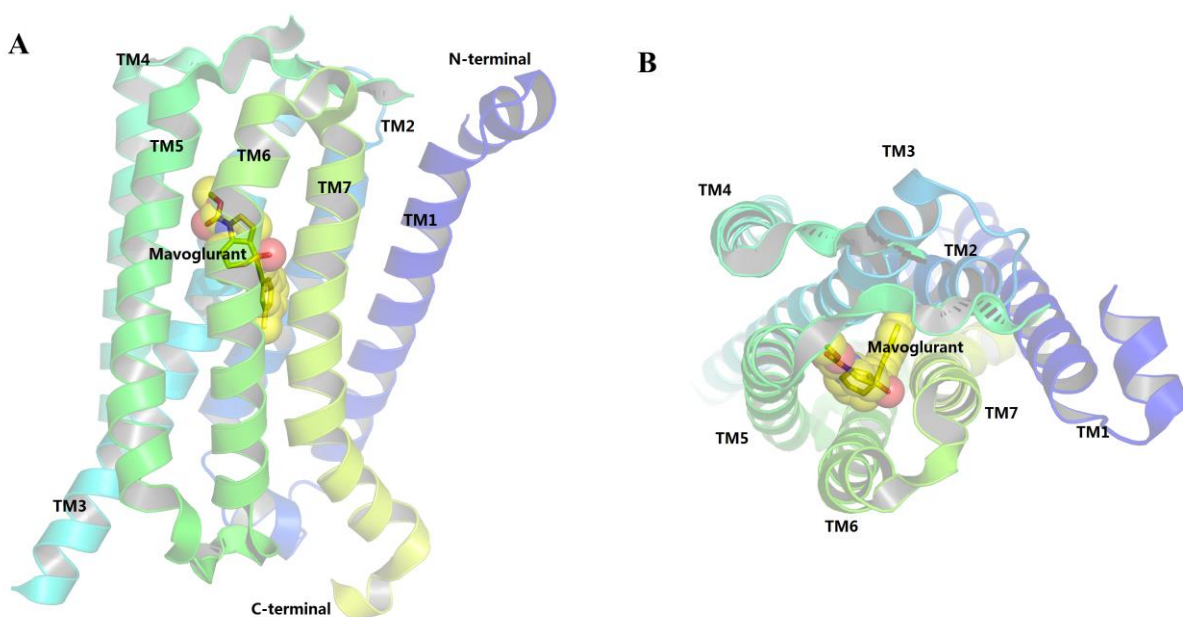


**Figure 3.** Crystalized structure of mGlu<sub>5</sub> transmembrane domain in complex with mavoglurant

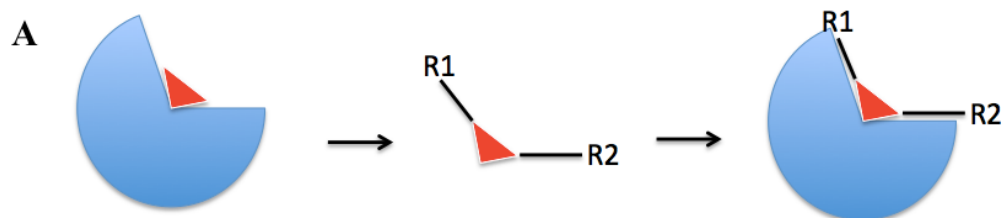
**A.** View from the membrane side. **B.** Top view from the extracellular side.

The structure shows that mavoglurant binds between helices 2, 3, 5, 6, 7 and make interactions with Ser805, Ser809, and Asn747. Multiple research groups have focused on the allosteric regulation of mGlu<sub>5</sub>, for example, Andreas Ritzén's group and P. Jefferey Conn's group designed and synthesized a series of allosteric ligands for mGlu<sub>5</sub>.(19) With the availability of the

crystal structure a classical structure-based medicinal chemistry approach could be useful for the generation of corresponding allosteric modulators, state-of-the-art computational methods could also be powerful tools in generating new ideas in allosteric modulator design in this field.(20, 21)

### 1.3 FRAGMENT-BASED DRUG DESIGN

Fragment-based approaches for designing and generating lead compounds have proven quite fruitful in drug discovery. There are several ways that fragment-based approach could be applied to drug discovery: (1) binding sites and pharmacophores identification for receptor binding could be achieved with fragment screening techniques; (2) HTS libraries could be biased and the optimization of lead compounds could be guided with fragments screening hits; (3) leads with the potential to be optimized into drug-like compounds can be identified with fragment screening.(21-25) Fragment binding can reveal hot spots on proteins, which could result in high-affinity receptor-ligand interactions. The fragment-based approach is especially suitable for detecting the interaction spots among the protein-ligand binding, as fragments are capable of interacting with a certain region of the target protein. Once the identification of fragments inside the binding pocket is done, these fragments could be grown, linked or merged to develop the potential ligands (**Figure 4**).(21)



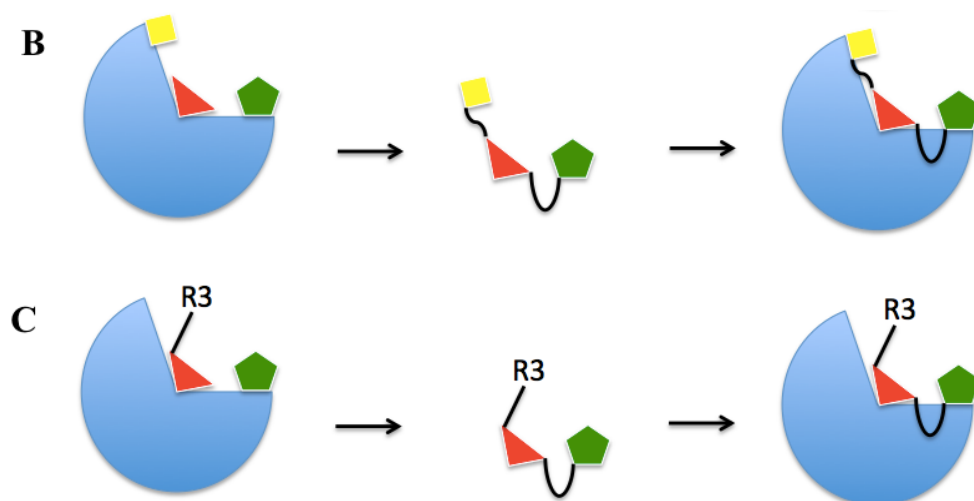


**Figure 4.** Commonly used strategies for fragment-based drug design

**A. Growing.** After identification of one suitable fragment inside the binding pocket, substitutions could be added to the identified fragment. The growing process would increase the lead likability of the original fragment to enhance the receptor-ligand interactions. **B. Linking.** Multiple fragments could be identified for one binding pocket simultaneously targeting at different regions. Linkers would be introduced to connect separated fragments to increase the lead likability, and to create a novel compound with potential affinity towards the pocket. **C. Merging.** A known lead could partially occupy the binding pocket. One or more fragment(s) could be identified to be suitable for the remaining space. One or more linker(s) could be introduced to connect the known lead and the fragment(s) to increase the strength of receptor-ligand interactions.

A number of fragment based screening campaigns have successfully delivered clinical candidates.<sup>(26)</sup> Steven Howard and his group successfully applied fragment-based screening and fragments linking to discover novel thrombin inhibitors.<sup>(27)</sup> Philip D. Edwards and his group reported the novel cyclic amidine  $\beta$ -secretase with the fragment-based approach to generate lead compounds.<sup>(28)</sup> However, there are still several undesired drawbacks for this approach. The

defects of the experimental fragment-based method include time consuming, costly, and low affinity of hits.(21, 29, 30) Another complementary way to approach fragment-based drug discovery is the application of computational methods, which can offer several advantages: (1) computational methodologies can construct high quality and diversified fragment libraries with both time and cost efficiencies;(31, 32) (2) computational approaches can easily explore larger fragment databases; (3) optimization strategies for improving the drug-likeness of the hits with computational tools have efficiency and flexibility.(33) Recently, a drug design effort, that involved virtual screening of a fragment library, binding confirmation by NMR, X-ray crystallography, and structure-based optimization of fragments, by a research group in AstraZeneca lead to the discovery of highly potent FXIa inhibitors(34). Another example is the development of inhibitors of cyclophilin A. Li's group reported that amide fragments, which functions as the key linker, is one of the critical pharmacophores for CypA inhibitors.(35) Through computational FBDD approaches, acylurea was designed by fusing amide and urea to function as a new linker and contributed to the discovery of novel inhibitors. Computational fragment-based drug design involves five major steps (**Figure 5**). First, the establishment of the diversified fragment library. Considering the advancement in computational power, a very large number of fragments can be screened in each experiment. This guarantees a good degree of fragment diversity and increases the statistical probability of finding suitable fragments for a given pocket. Second, virtual screening of the fragment library to find suitable fragments. Fragments are relatively small compounds, which would not likely give appealing binding energies or docking scores during the docking process. However, analysis of the potential receptor-ligand interactions, like H-bond or hydrophobic interactions, suitable fragments could be identified. Third, design the lead compounds based on identified fragments. As mentioned above, fragment growing,

fragments linking, and lead-fragments merging are strategies that can be used in this step. Fourth, the verification of generated novel leads with corresponding biological assays. Computational validation methods would be applied at the beginning to filter out false positives or false negatives. Corresponding biological assays would be followed to formally verify the effectiveness of these lead compounds. Fifth, NMR confirmation of binding. The last step mainly contributed to the mechanism understanding. After the growing, linking, or merging steps, fragments inside a compound may not recur at the identical places from the virtual screening. Confirming the binding mode of the compounds with NMR would reveal receptor-ligand interactions and provide insight for the mechanism of receptor activation or inhibition.

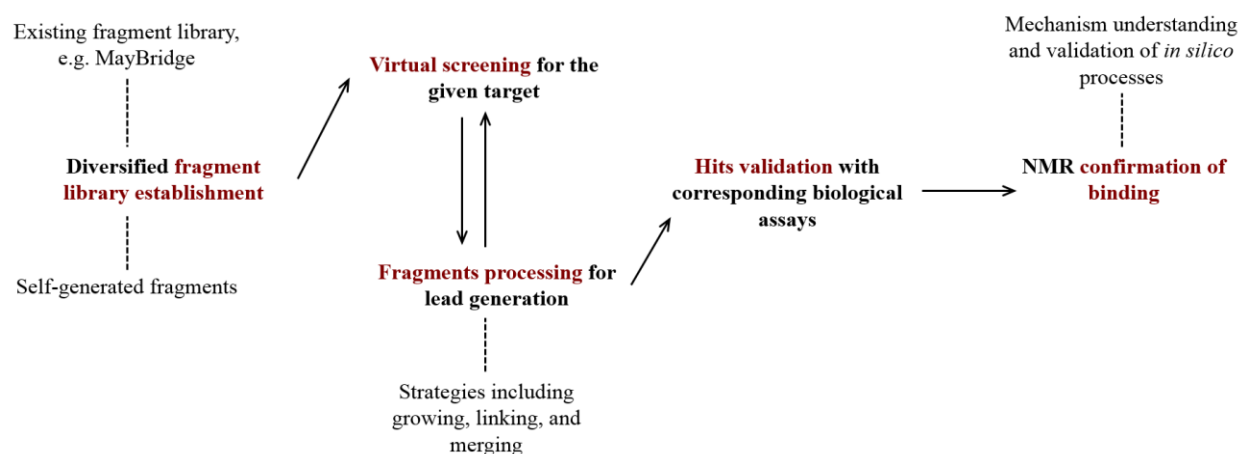


**Figure 5.** Flowchart of computational fragment-based drug design

Five major steps are considered. First, the establishment of diversified fragment library. Second, the virtual screening for the given target. Third, the fragments processing for the lead generation. Fourth, the hits validation with biological assays. Fifth, the confirmation of binding mode.

In our research, we use a computational fragment-based approach to propose structures as potential novel allosteric modulators of mGlu<sub>5</sub>. We generated a fragment library from the reported GPCRs' allosteric modulators on Allosteric Database (ASD v2.0).(36) Retrosynthetic combinatorial analysis procedure (RECAP) analysis and synthesis were used to generate the novel compounds. Molecular docking was applied to screen the hits for mGlu<sub>5</sub> by docking the *in silico* synthesized compounds back to the pocket and predicted binding energy and docking scores. Computational methodologies, such as benchmark dataset verification, docking studies, QuaSAR model, etc. were utilized for further validation of our hits. 20 *in silico* synthesized compounds are predicted to be potential mGlu<sub>5</sub> allosteric modulators with preferable binding energies and docking scores. Structure diversity among the *in silico* design could be observed. Series of compounds with reported allosteric activities on mGluR could be recurred. Our case study on designing allosteric modulators on mGlu<sub>5</sub> suggested that this computational fragment-based approach is a useful methodology for facilitating the future compounds design processes.

## **2.0 MATERIALS AND METHODS**

### **2.1 X-RAY STRUCTURES AND GPCR ALLOSTERIC MODULATORS**

Two x-ray structures of transmembrane domain of the human mGlu<sub>5</sub> were used in this work. The first model (PDB entry: 4OO9; resolution, 2.6 Å; method, X-ray diffraction)(16) was in complex with the negative allosteric modulator, mavoglurant. The second model (PDB entry: 5CGD; resolution, 2.6 Å; method, X-ray diffraction)(37) was in complex with the negative allosteric modulator, HTL14242. The structures of mGlu<sub>5</sub> were downloaded from the Protein Data Bank



(PDB). SYBYL-X 1.3(38) was used for the preparation of the crystal structures, including energy minimization and residues repair.(39)

Ligands downloaded from the Allosteric Database (ASD v2.0)(36) SYBYL-X 1.3 and PyMol (<http://www.pymol.org>) were used for molecular visualization, structural superimposition, and data analysis.(40)

## **2.2 FRAGMENTS GENERATION AND *IN SILICO* SYNTHESIS**

The RECAP Analysis and RECAP Synthesis tools in the ChemAxon's Fragmenter software (<https://www.chemaxon.com>) were used for the establishment of the fragment library from allosteric modulators in ASD and the generation of *in silico* synthesized novel structures from processed, analyzed, and categorized fragments. The Molecule Filter was set to be Leadlike.(41) The Heavy Atoms were set to be 25 in average with 11 in standard deviation. The purpose of RECAP Analysis is to fragment compounds according to simple retrosynthetic analysis rules and gather statistics towards fragments products. The RECAP Synthesis could be applied to combine fragments products from RECAP Analysis randomly, in order to produce the novel chemical structures, which should be synthetically reasonable.(42, 43) .

## **2.3 MOLECULAR DOCKING FOR THE STUDIES OF mGlu<sub>5</sub>-LIGAND INTERACTIONS**

We performed the molecular docking between crystal structure of mGlu<sub>5</sub> and fragments in the fragment library using SYBYL-X 1.3. Surflex-Dock GeomX, the docking algorithm that

implemented in SYBYL, was applied to predict detailed receptor-ligands interaction. The Total Score was expressed as  $-\log_{10}(K_d)$ .(44) In the docking simulations, the allosteric binding site was first defined to cover all residues within 4 Å of the NAM in the initial mGlu<sub>5</sub>-mavoglurant complex. The Kollman all-atom approach was used to calculate atomic charges for the protein(45) and the Gasteiger-Hückel approach for the ligand.(46) The movement of hydrogen atoms of the protein was allowed. Additional starting conformations per molecule were set to 10, and the angstroms to expand search grid was set to 6. Three independent runs were performed for our fragment library.

Molecular docking between the *in silico* synthesized compounds was done with SYBYL-X 1.3 and AutoDock 4.0(47). The parameters stated above of SYBYL-X 1.3 were used in these docking experiment. For AutoDock, Lamarckian genetic algorithm (LGA),(48) was used in this study. The grid box contained the entire allosteric binding site of the mGlu<sub>5</sub> and permitted translation and rotation of ligands. Numbers of points in Grid box for three dimensions were 24, 24 and 22; spacing (angstrom) was 1.000. AutoGrid was used for calculating the energy map of each atom in the ligands. The receptor was set to be rigid. Genetic algorithm with default parameters was chosen for the search. A binding energy, which is constituted by intermolecular energy, internal energy, torsional energy and unbound extended energy, was reported for each run.

## 2.4 GENERATION OF BENCHMARKING DATASET

Enrichment of top hits was key metric for docking studies.(49) Once a docking screening could distinguish active compounds as top hits against a large number of decoys in the database, this docking screening is considered a success.(50) In order to distinguish the *in silico* synthesized compounds from decoys in the docking processes a benchmarking dataset is introduced. In the

spirit of the DUD(49) and DUD-E(51) reference data sets for validation studies, 50 decoys, which have similar physical properties but distinctive topological properties with the reported mGlu<sub>5</sub> NAM were generated through <http://decoys.docking.org>, using the reported protocols and parameters.

## 2.5 QUANTITATIVE STRUCTURE-ACTIVITY RELATIONSHIP MODEL

The correlation between the structures of molecules and their corresponding chemical or physical properties could be summarized and predicted with Quantitative structure-activity relationships (QSAR) techniques.(52) A QSAR model could be used to evaluate specific parameters that affecting some properties of the molecules or to estimate same properties for other molecules in the same series.(53) A QSAR model, dealing with the correlation between the Log*K<sub>i</sub>* value and theoretical descriptors for molecules, was developed using 66 analogs of 1,2-diphenylethyne mGlu<sub>5</sub> NAMs with existing *K<sub>i</sub>* values in ASD. *K<sub>i</sub>* values underwent logarithmic transformation to get Log*K<sub>i</sub>* values. Kennard-Stones algorithm was used for determining the training and test sets. 186 descriptors were added towards each compound. Four criteria, contingency coefficient, Cramer's V, entropic uncertainty, and linear correlation were used to evaluate the contribution of each descriptor after the contingency analysis.(54-56) Partial least squares (PLS) regression method was used for building the model with selected descriptors. The model has been verified with the test set and used for the prediction of *in silico* synthesized compounds.

## 3.0 RESULTS

### 3.1 STUDY DESIGN AND THE STRATEGIES FOR DESIGNING NOVEL COMPOUNDS

In designing new leads we followed the workflow described in **Figure 6**. First, we constructed a diversified fragment library from GPCR allosteric modulators in ASD using RECAP Analysis. Docking studies between the mGlu<sub>5</sub> allosteric pocket and fragment library were followed. Despite the relatively weak interactions between the fragments and the surrounding residues, the aggregation of fragments in different regions inside the pocket could be observed and analyzed. Then, fragments linking was adopted as the strategy for processing the fragments, based on their spatial positions inside the pocket. After the generation of lead compounds, docking studies between newly created lead compounds and the mGlu<sub>5</sub> allosteric pocket were performed to identify hits. Finally, multiple docking algorithms, enrichment test, and QSAR model simulation were combined to virtually validate the effectiveness of selected hits. 20 *in silico* synthesized compounds were reported to be potential mGlu<sub>5</sub> allosteric modulators. Details are described in the following paragraphs.

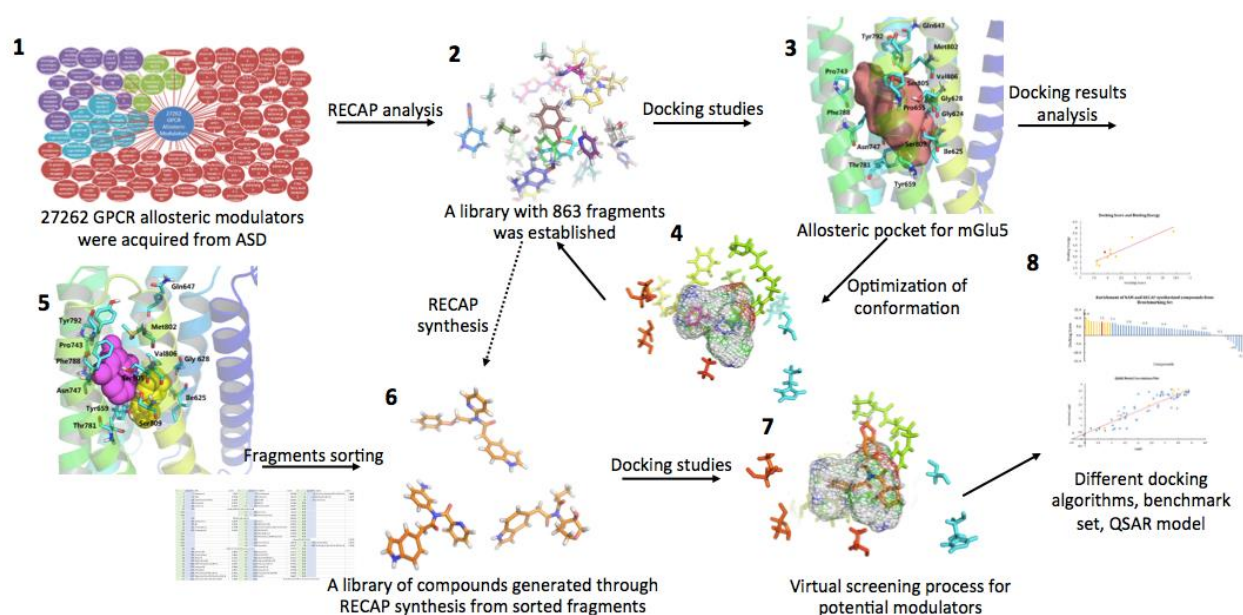


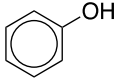
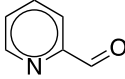
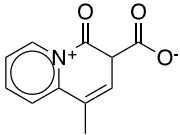
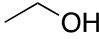
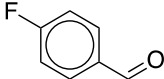
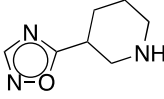
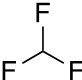
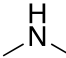
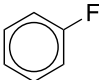

**Figure 6.** Study design and strategies for designing novel mGlu5 allosteric modulators

### 3.2 THE ESTABLISHMENT OF FRAGMENT LIBRARY

27262 GPCR allosteric modulators were downloaded from ASD. RECAP Analysis in ChemAxon's Fragmenter (<https://www.chemaxon.com>) was used to generate our fragment library. "Rule of three"(57, 58) rather than "Rule of five"(59) was used here for guiding the selection of ideal fragments. The contents for "Rule of three" included molecular weight < 300, hydrogen bond donors  $\leq 3$ , hydrogen bond acceptors  $\leq 3$ , and cLogP  $\leq 3$ . After deleting duplicate items, a library with 863 fragments was generated. Among them, 47 fragments had molecular weights over 300; 3 fragments had over 3 hydrogen bond donors; 56 fragments had over 3 hydrogen bond acceptors; and 72 fragments had their LogP(o/w) values over 3. **Table 2** demonstrates top ten most frequently appeared fragments with corresponding properties as an example. A comparison between the fragment library we generated and the Maybridge fragment library was conducted. MACCS Structural Keys were used for calculating the fingerprint of each

fragment. Tanimoto Coefficient was set to be 80%. 78% of fragments in the library we generated could be matched with items in Maybridge library, while the remaining 22% of fragments may contribute to the particularity of GPCR allosteric modulators.

**Table 2.** Structure and properties for top ten most frequently appeared fragments

Structure	Frequency	LogP(o/w)	M.W.	Hydrogen bond donor	Hydrogen bond acceptor
	407	1.60	94.11	1	1
	357	0.56	107.11	0	2
	324	0.91	203.20	0	1
	197	-0.06	46.07	1	1
	188	1.99	124.11	0	1
	188	-0.42	153.19	1	3
	173	0.99	70.01	0	0
	167	-0.10	45.08	1	1
	163	2.06	96.10	0	0
	162	0.67	79.10	0	1

### 3.3 DOCKING STUDIES OF FRAGMENTS INTO mGlu<sub>5</sub>

Before docking studies of the fragments we docked the reported NAM, mavoglurant, back to the defined allosteric binding site to function as a control for the validation of our docking process. Residues from TM2, TM3, TM5, TM6 and TM7 formed the pocket. Gly624, Ile625, Gly628, Pro655, Ser805, Val806, and Ser809 were directly involved in the pocket (**Fig. 7A**). Comparing our docking results with the crystal structure of human mGlu<sub>5</sub> (PDB entry: 4OO9; resolution, 2.6 Å; method, X-ray diffraction)(16) in complex with the negative allosteric modulator, mavoglurant bound well inside the pocket with the alkyne linker traversing a narrow channel between Tyr659, Ser809, Val806, and Pro655. Three hydrogen bonds could be formed between mavoglurant and Asn747, Ser805, Ser809 (**Fig. 7B**). Our docking studies between mavoglurant and the defined allosteric binding site provided congruent results with the crystal structure. Identical residues were involved in the formation of hydrogen bond interaction (**Fig. 7C**). The docking result overlapped well with the crystallized complex, with the RMSD of ~0.3Å (**Fig. 7D**), indicating that our docking process is relatively reliable.

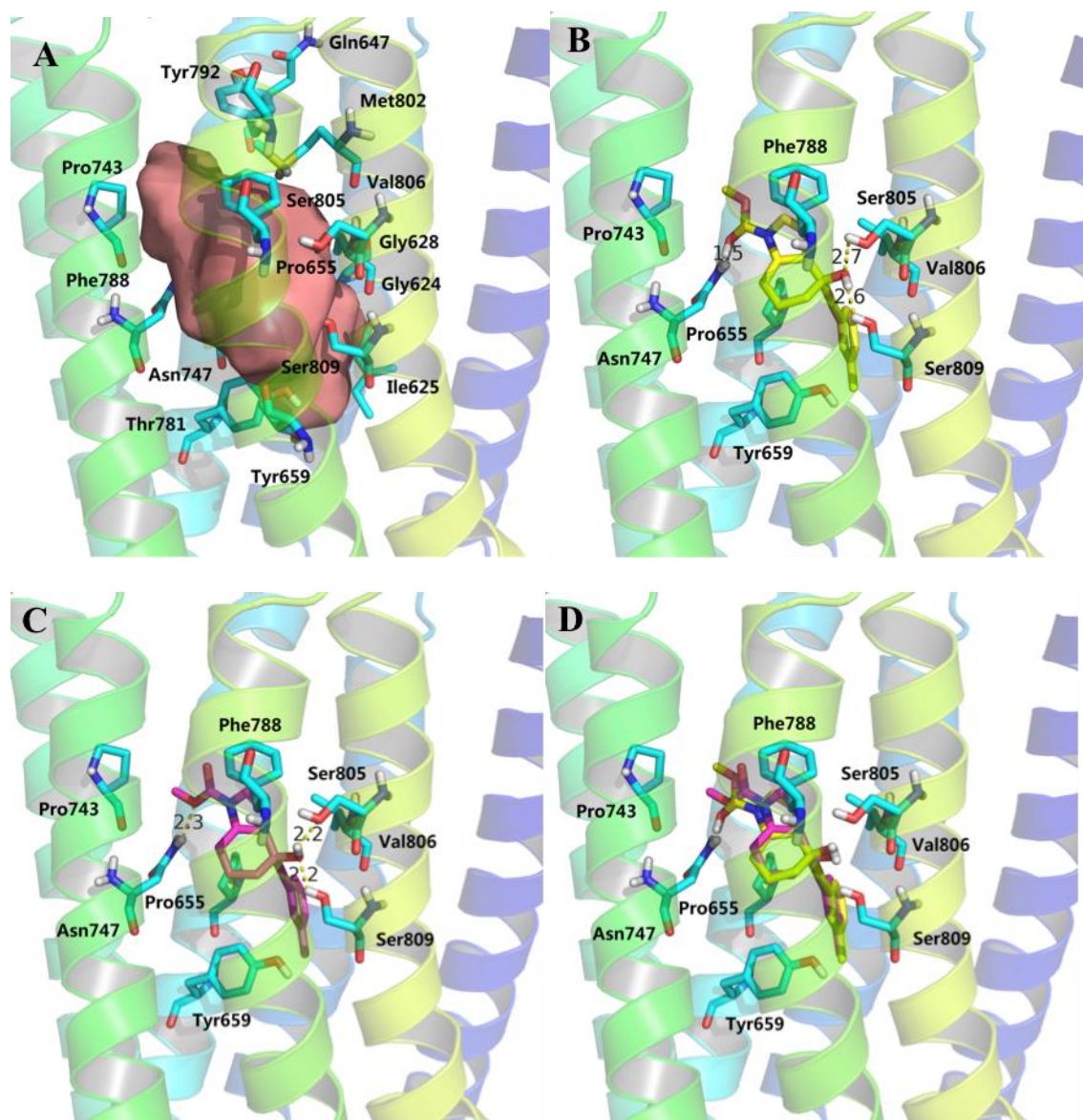


**Figure 7.** Allosteric binding site of mGlu<sub>5</sub>

**A.** The allosteric binding site (highlighted in salmon pink), which is formed by surrounding residues marked in cyan. **B.** The interaction between mavoglurant and surrounding residues based on the spatial information from the reported crystal complex. **C.** Docking pose and ligand-residue interaction predicted through the docking study. **D.** The overlap of mavoglurant between crystallized complex and predicted pose.



Then the generated fragments in our fragment library were docked into the mGlu<sub>5</sub> allosteric binding site. We conducted three independent docking studies for all fragments, and found that fragments invariably aggregated into two distinct regions of the binding pocket of mGlu<sub>5</sub>, an upper region and a bottom region (**Figs. 8A and 8B**).

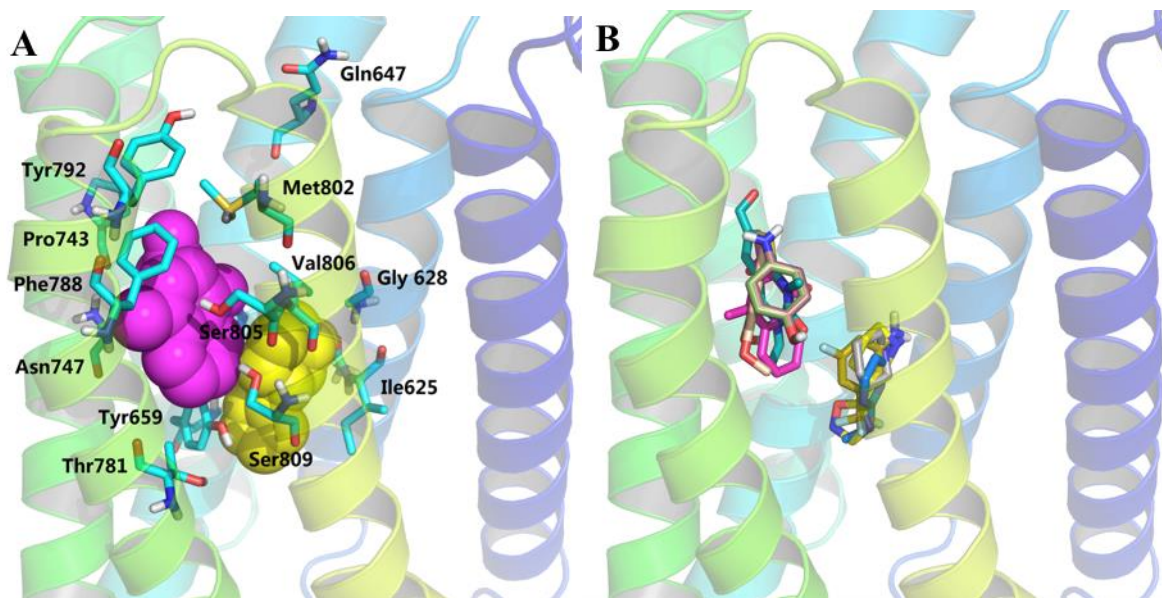


**Figure 8.** Fragment docking studies

**A.** Upper region (highlighted in pink) and bottom region (highlighted in yellow), which are connected through a narrow channel and recognized through fragments docking. **B.** The aggregation of fragments inside the allosteric binding site.

The number of fragments for each region was summarized in **Fig. 9**. Our docking results were very consistent across our three independent runs, with ~416 (85%) of fragments in the upper region and ~320 (87%) of fragments in the bottom region were repeated in the same region throughout the three docking runs.

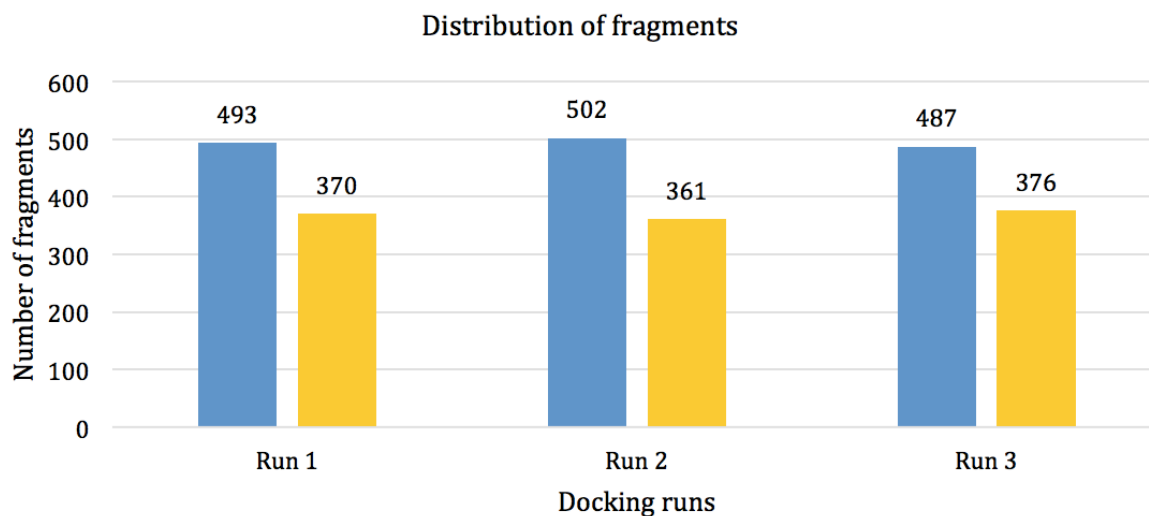


**Figure 9.** Fragments sorting

The distribution of fragments towards the upper and bottom regions from three independent docking runs.

### **3.4 *IN SILICO* SYNTHESIS OF NOVEL COMPOUNDS FROM CATEGORIZED FRAGMENTS**

A single fragment may bind with low affinity to a protein because of the lower molecular weight, which results in a limited amount of ligand-receptor interaction.<sup>(60)</sup> The combination of the fragments from upper and bottom regions is a promising strategy for increasing the affinity of binding. RECAP Synthesis in ChemAxon Fragmenter was used to combine the fragments in upper region with the fragments in the bottom region. In order to find out whether the docking scores can be used as guidance for RECAP Synthesis, a trial was first conducted. A small scale of RECAP Synthesis was performed with two sets of fragments: (1) ~600 compounds were generated by 30 fragments in upper region and 20 in bottom region with the highest docking scores; (2) ~600 compounds were generated by 30 fragments in upper region and 20 in bottom region with the

lowest docking scores, respectively. The distribution of their docking scores (**Fig. 10**) revealed that the combination of fragments with higher docking scores tended to result in compounds with better binding affinities. The Mann-Whitney Test showed that asymptotic significance (2-tailed) is less than 0.001, which meant these two distributions were significantly different.

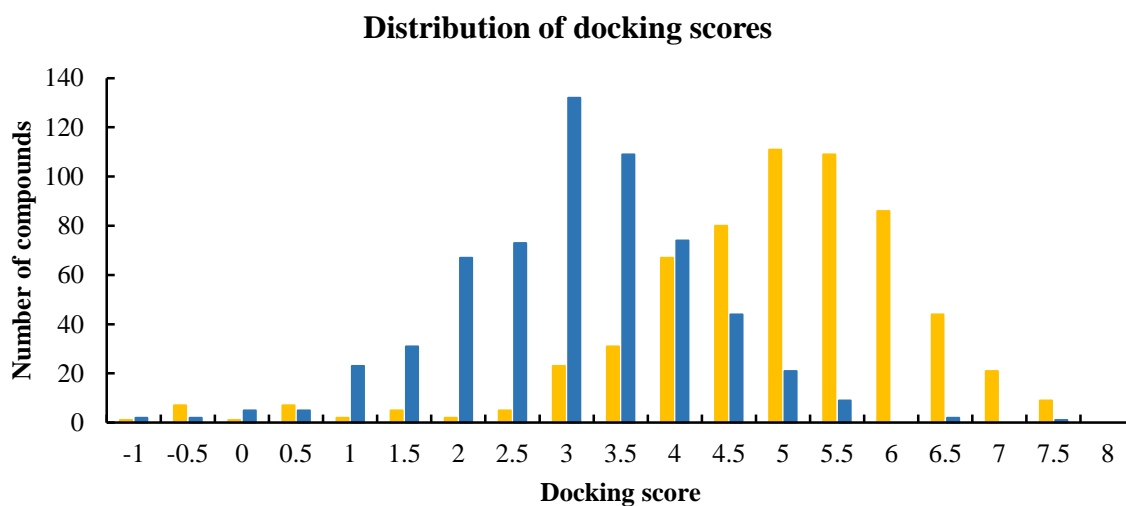


**Figure 10.** Distribution of the docking scores for small scale RECAP Synthesis

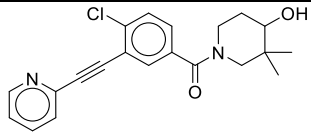
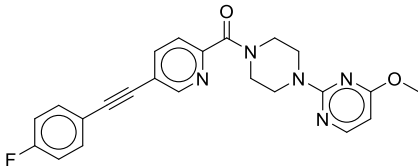
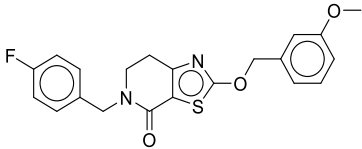
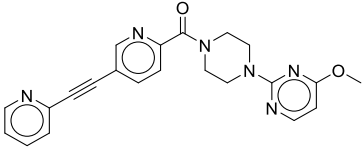
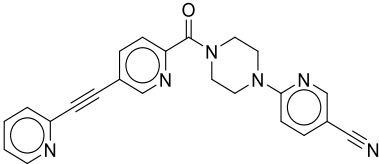
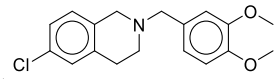
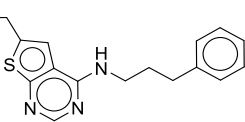
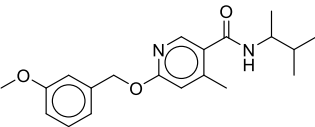
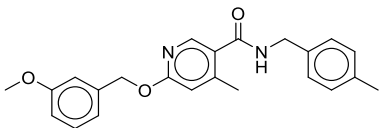
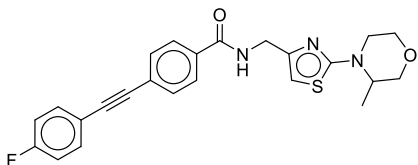
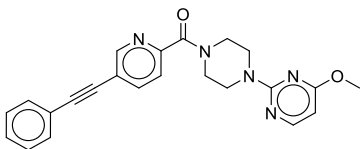
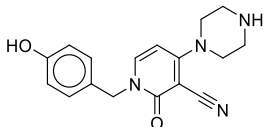
Yellow bars represent compounds generated from fragments with highest docking scores. Blues bars represent compounds generated from fragments with lowest docking scores. Two-tailed Mann-Whitney Test was performed to prove the significant difference between these two distributions.

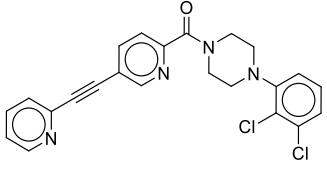
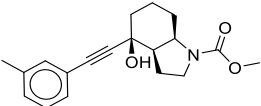
Then, 9600 novel compounds were generated through the large-scale RECAP Synthesis with 120 highest scored fragments in the upper region (**Supplementary Table. 1**) and 80 highest scored fragments in the bottom region (**Supplementary Table. 2**). Our results showed that 124 *in silico* synthesized compounds had the docking score higher than seven (**Supplementary Table. 3**). Since the docking score was expressed as  $-\log_{10}(K_d)$ , as described in **Materials and Methods**,

compound with a docking score higher than seven means that their corresponding predicted  $K_i$  is less than  $10^{-7}$  Mol, which is a positive sign for binding affinity. Interestingly, six *in silico* synthesized compounds have higher docking scores than mavoglurant. The structures of top 20 *in silico* synthesized compounds, as well as the mavoglurant, were shown in **Table 3**.

**Table 3.** Docking score, binding energy and predicted  $K_i$  value for top 20 *in silico* synthesized compounds.

No.	Structure	Docking score	Binding energy	Predicted $K_i$
1		10.4	-7.7 kcal/mol	1.3 nM
2		8.9	-7.2 kcal/mol	10.9 nM
3		8.3	-5.5 kcal/mol	67.3 nM
4		8.1	-6.1 kcal/mol	132.6 nM
5		8.1	-5.8 kcal/mol	88.1 nM
6		8.0	-5.4 kcal/mol	324.2 nM
7		7.7	-4.7 kcal/mol	545.0 nM

8		7.6	-5.1 kcal/mol	225.5 nM
9		7.6	-4.8 kcal/mol	199.4 nM
10		7.6	-5.4 kcal/mol	--
11		7.6	-5.3 kcal/mol	207.0 nM
12		7.5	-4.5 kcal/mol	130.9 nM
13		7.5	-4.3 kcal/mol	--
14		7.4	-4.4 kcal/mol	--
15		7.4	-5.5 kcal/mol	--
16		7.4	-5.1 kcal/mol	--
17		7.3	-4.2 kcal/mol	1162.3 nM
18		7.3	-5 kcal/mol	357.6 nM
19		7.3	-4.1 kcal/mol	--

<b>20</b>		7.3	-4.4 kcal/mol	792.2 nM
<b>NAM</b>		7.9	-5.9 kcal/mol	107.0 nM (Experimental Ki value: 66 nM)

Moreover, we introduced binding energy of molecular docking as a supplementary evidence for receptor-ligand interaction by using AutoDock 4.0. The results of top 20 compounds can be found in **Table 3**. A correlation plot was drafted (**Fig. 11**) to show the relationship between the docking score and the binding energy for each compound. All of these 20 *in silico* synthesized compounds had a predicted negative binding energy, which had a high correlation with the docking scores, (61, 62) providing the evidence that the docking studies with SYBYL-X 1.3 and AutoDock 4.0 were consistent with each other.

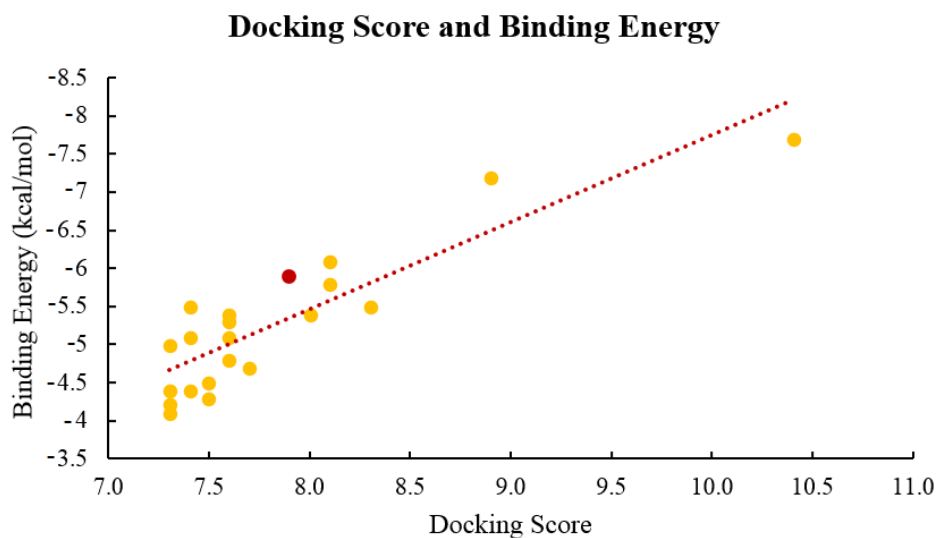


**Figure 11.** Correlation plot for docking score and binding energy

Red spot represents the docking score and binding energy for mavoglurant. Yellow spots represent the docking scores and binding energies for 20 *in silico* synthesized compounds.

The binding poses of the highest ranked *in silico* synthesized compound was compared with the reported NAM, mavoglurant. The *in silico* synthesized compound occupied the identical position as mavoglurant (**Fig. 7B**), forming the hydrogen bond with Ser805 (**Fig. 12A**). Two compounds overlapped very well with the RMSD of 1 Å, as shown in **Fig. 12B**. Interestingly, our docking studies suggest that compound 1, our highest scoring compound proposed by our *in silico* methods, is predicted to form hydrogen bonds with Thr735 and Tyr659, which are not reported for mavoglurant. These two additional receptor-ligand interactions might explain the higher docking score acquired by the highest ranked *in silico* synthesized compound than mavoglurant. Whether or not these would actually form if compound 1 were synthesized and crystallization attempted would be an interesting experiment to conduct.

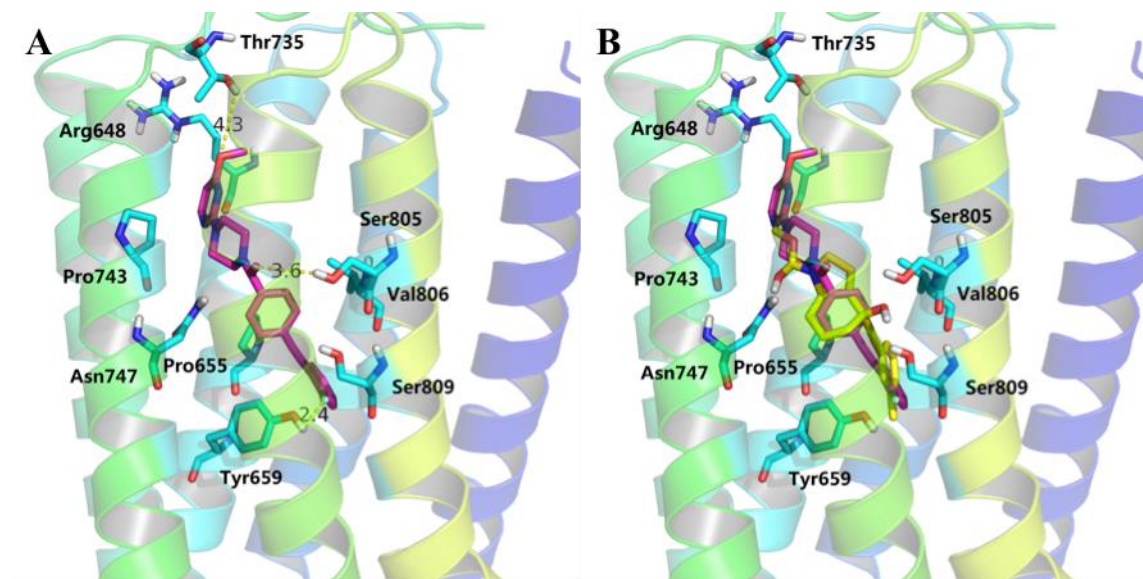


**Figure 12.** *In silico* synthesis of potential mGlu<sub>5</sub> allosteric modulators

**A.** The binding pose of top one *in silico* synthesized compound. **B.** Comparison of binding poses between top one *in silico* synthesized compound (pink) and mavoglurant (yellow).

### 3.5 ENRICHMENT TEST WITH A BENCHMARKING DATASET

Dr. John. J. Irwin and his group generated the Directory of Useful Decoys, Enhanced (DUD-E), which is available at <http://dude.docking.org>. The physical properties used are molecular weight, calculated LogP, H-bond donors and acceptors, the number of rotatable bonds and net molecular charge in order to build physically similar decoys.<sup>(51)</sup> A tool (<http://decoys.docking.org>), which is automated and available online could be used for generating the matched decoys for user-supplied ligands. The reported mGlu<sub>5</sub> NAM, mavoglurant, was used as the ligand for decoys generation. 71 compounds, including 50 decoys (**Supplementary Table. 4**), mavoglurant, as well as top 20 *in silico* synthesized compounds were docked into mGlu<sub>5</sub> (**Fig. 13**). Our results showed a clear enrichment of NAM and *in silico* synthesized compounds against 50 decoys. These results indicated that 20 *in silico* synthesized compounds could be enriched with NAM, and were different from challenging decoys.



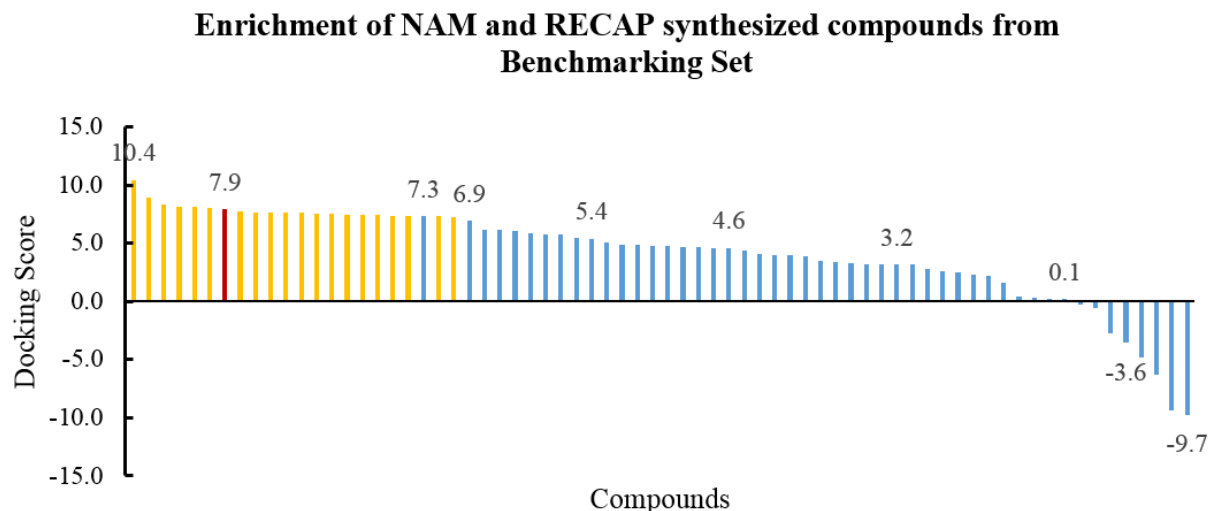


**Figure 13.** The enrichment test with decoys

The red bar represents the reported negative allosteric modulator, mavoglurant, for mGlu5. Yellow bars represent the top 20 in silico synthesized compounds. Blue bars represent the decoys generated under DUD-E.

### 3.6 PREDICTION OF COMPETITION BINDING WITH A QUANTITATIVE STRUCTURE-ACTIVITY RELATIONSHIP MODEL

The selectivity of a ligand towards receptor subtypes could be measured with the competitive binding assay, which also reveals the percentage and density of each subtype among a certain tissue.<sup>(63)</sup> Competition binding is widely used in testing potential allosteric modulators for GPCRs. 66 analogs of 1,2-diphenylethyne with existing  $K_i$  values were selected from ASD (**Supplementary Table. 5**). Following the method described in the *Materials and Methods*, a QSAR model with 12 descriptors was built:

$$\begin{aligned} \text{LogKi} = & -6.81 + 3.11 * \text{BCUT\_PEOE\_3} - 2.46 * \text{BCUT\_SLOGP\_3} + 0.46 * \text{b\_1rotN} - 12.76 * \\ & \text{b\_1rotR} - 9.57 * \text{GCUT\_PEOE\_0} - 4.37 * \text{GCUT\_SLOGP\_0} + 4.49 * \text{GCUT\_SMR\_0} - 0.17 * \\ & \text{Kier3} + 0.06 * \text{PEOE\_VSA+5} - 0.03 * \text{SlogP\_VSA4} - 0.02 * \text{SMR\_VSA0} - 0.02 * \text{SMR\_VSA1} \end{aligned}$$

**Table 4.** Descriptors of linear regression analysis

Notation	Descriptors	Coefficient	Contingency coefficient	Cramer's V	Entropic uncertainty	Linear correlation
Intercept	-	-6.81	-	-	-	-
BCUT_PEOE_3	PEOE Charge BCUT (3/3)	3.11	0.82	0.41	0.43	0.16
BCUT_SLOGP_3	LogP BCUT (3/3)	-2.46	0.80	0.39	0.40	0.17
b_1rotN	Number of rotatable single bonds	0.46	0.69	0.27	0.22	0.15
b_1rotR	Fraction of rotatable single bonds	-12.76	0.79	0.37	0.36	0.20
GCUT_PEOE_0	PEOE Charge GCUT (0/3)	-9.57	0.81	0.40	0.44	0.29
GCUT_SLOGP_0	LogP GCUT (0/3)	-4.37	0.77	0.35	0.39	0.17
GCUT_SMR_0	Molar Refractivity GCUT (0/3)	4.49	0.82	0.41	0.41	0.20
Kier3	Third Kappa shape index	-0.17	0.76	0.33	0.30	0.19
PEOE_VSA+5	Total positive 5 vdw surface area	0.06	0.66	0.25	0.30	0.19
SlogP_VSA4	Bin 4 SlogP (0.10, 0.15)	-0.03	0.78	0.36	0.36	0.20

SMR_VSA0	Bin 0 SMR (0.000, 0.110)	-0.02	0.72	0.30	0.32	0.16
SMR_VSA1	Bin 1 SMR (0.110,0.260)	-0.02	0.73	0.31	0.28	0.25

**Table 4** shows the calculated descriptors for each molecule, the descriptors coefficients, contingency coefficient, Cramer's V, entropic uncertainty, and linear correlation. A correlation plot between the predicted  $\text{Log}K_i$  values and experimental  $\text{Log}K_i$  values was shown in **Fig. 14**. With a correlation coefficient of 0.82 and a cross-validated correlation coefficient of 0.74, the established QSAR model was acceptable.<sup>(64)</sup> This model was used to predict the  $K_i$  values for 14 compounds among the top 20 *in silico* synthesized compounds, as listed in **Table 3**. Compounds 10, 13-16, and 18 were excluded from the prediction with this QSAR model, because they have distinctive structural features towards 1,2-diphenylethyne analogs. The predicted values for 14 compounds are ranging from 1.3 nM to 1162.3 nM. Although discrepancies do exist, generally speaking, these data are congruent with their docking scores and binding energies, indicating that these compounds are potential mGlu<sub>5</sub> allosteric modulators.

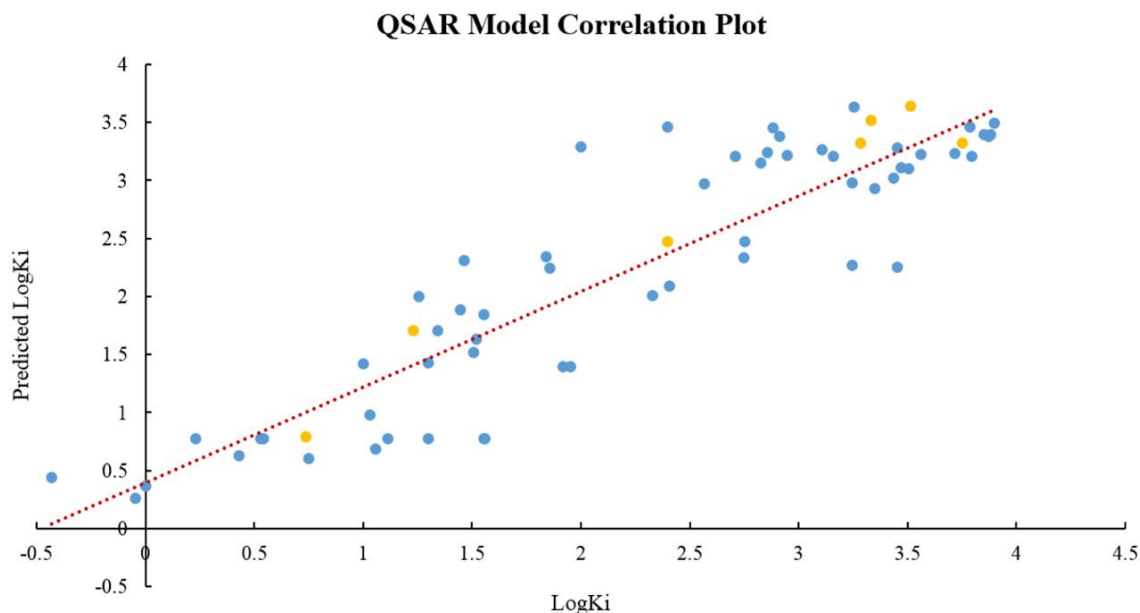


**Figure 14.** Correlation plot for quantitative structure-activity relationship model

Blue spots represent for items in training set. Yellow spots represent for items in test set. The root mean square error is 0.49. The correlation coefficient is 0.82. The cross-validated RMSE is 0.60. The Cross-validated R<sup>2</sup> is 0.74.

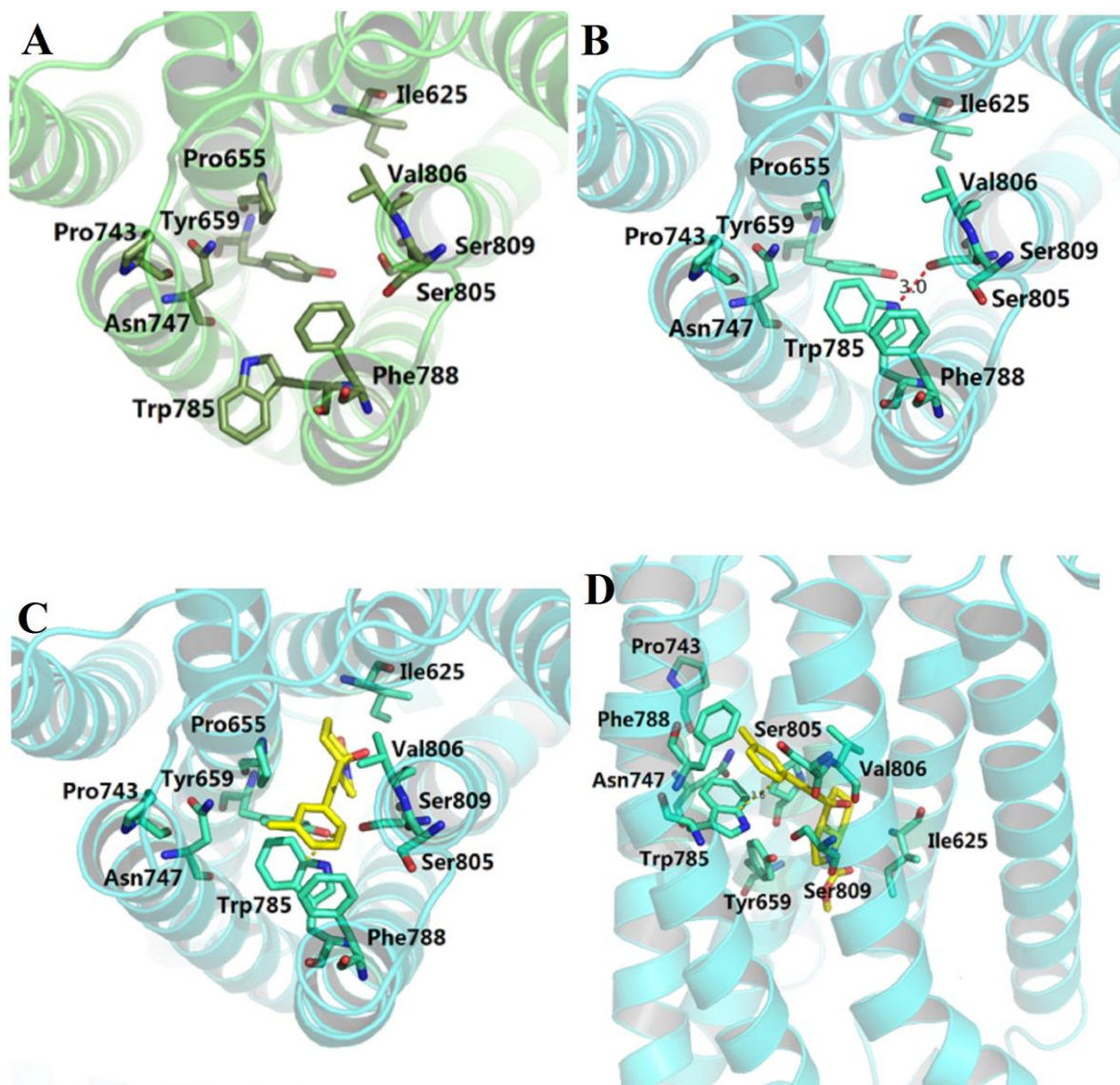
### 3.7 VALIDATION WITH PAINS-REMOVER AND TOXTREE

PAINS-Remover is designed and constructed to remove the Pan Assay Interference Compounds (PAINS) from screening libraries.<sup>(65)</sup> The top 20 *in silico* synthesized compounds listed in **Table 3** were tested by “Pan Assay Interference Compounds” (PAINS, [www.cbligands.org/PAINS/](http://www.cbligands.org/PAINS/)), and all compounds passed the filter. Toxtree (<http://toxtree.sourceforge.net/index.html>) is a software to estimate the toxic hazard through decision tree approach.<sup>(66)</sup> All these top 20 *in silico* synthesized compounds were tested with Toxtree, and all of them had the same level of estimated toxic hazard with the reported NAM, mavoglurant.

### 3.8 THE EFFECTS ON LIGANDS AND FRAGMENTS BINDING CAUSED BY THE ROTATION OF TRP785

The Trp785 on TM6 is highly conserved, which is similar to the central toggle switch in class A GPCRs. The different conformations of Trp785 could be observed between different crystal models due to the cocrystallization with different chemotypes. John A. Christopher and his group cocrystallized the mGlu<sub>5</sub> with HTL14242 and another molecule in the series in 2015. Their crystal model of mGlu<sub>5</sub> (PDB entry: 5CGD) has a different Trp785 conformation (**Figs. 15A and 15A**). The evaluation of ligands and fragments binding between these two models were performed to illustrate the effects caused by the rotation of a critical residue Trp785. Trp785 rotates out of the allosteric binding pocket on 4OO9, which results in a relatively large pocket, especially for the upper region (**Fig. 15A**). While for 5CGD, the Trp785 rotates into the allosteric binding pocket, which narrows down the space inside. One hydrogen bond could be formed between Trp785 and Ser809 in 5CGD, which further limits the size of the substructures for ligands to the top (**Fig. 15B**). The docking study between the mavoglurant and 5CGD shown that the saturated bicyclic ring system was no longer favored in the upper region due to the severe collision with Trp785. Instead, the aromatic ring on mavoglurant was placed in the upper region with potential hydrophobic interactions with rings system on Trp785, and the saturated bicyclic ring system was placed in the bottom region (**Figs. 15C and 15D**). This pose of mavoglurant was not favored by the allosteric binding pocket with a docking score of 4.5. The docking studies between 5CGD and 80 highest scored fragments in the bottom region, as well as 120 highest scored fragments in upper region were followed. The aggregation of fragments in the bottom region remained relatively well. **Fig. 15E** shows that the rotation of Trp785 has limited influence on the fragments aggregation in the

bottom region. Although some big fragments may invade into the upper region, the same situations could be observed with 4OO9, because of the size of these big fragments. **Fig. 15F** shows that the aggregation of fragments in the upper region can no longer be maintained, especially for big fragments. The fragments that used to be categorized in the upper region tend to distribute among both upper and bottom regions in 5CGD.



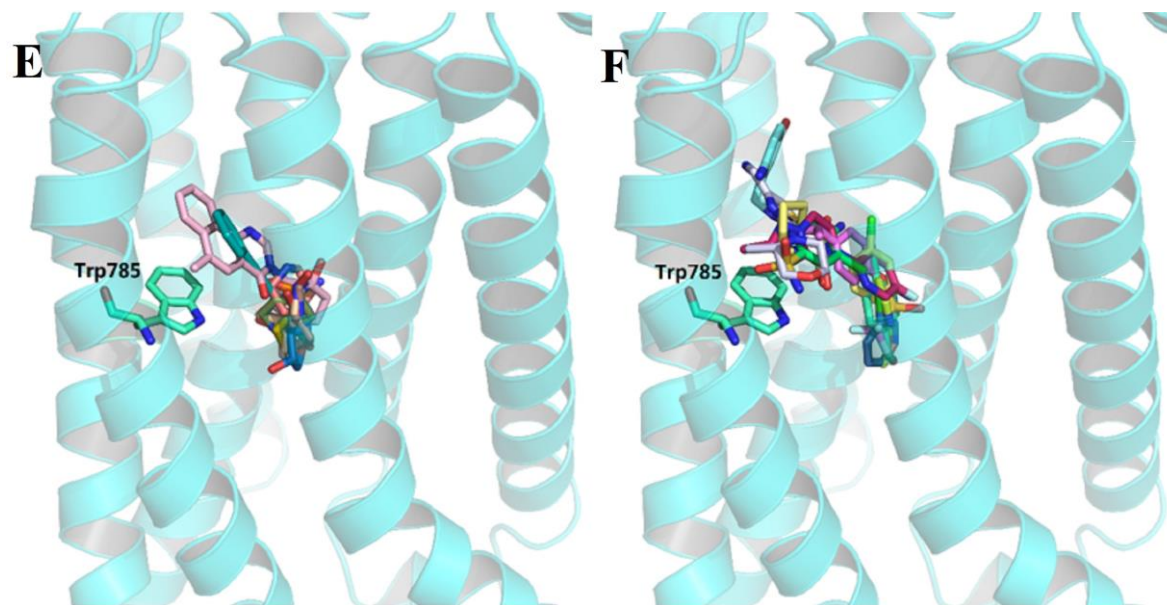


**Figure 15.** Assessment on the rotation of Trp785

**A.** Extracellular view on the mGlu<sub>5</sub> allosteric binding pocket from 4OO9. **B.** Extracellular view on the mGlu<sub>5</sub> allosteric binding pocket from 5CGD. **C. D.** Extracellular view and parallel to the membrane view on the binding pose of mavoglurant inside 5CGD according to the molecular docking. **E. F.** Distribution of categorized fragments in the allosteric binding pocket of 5CGD.

The distribution of fragments (**Fig. 16**) shown that the bottom region is favored by the majority of the fragments. Although the overall properties of the upper region remain hydrophobic, but the rotation of Trp785 significantly affects the shape of the upper region. The dramatic conformational changes on critical residues would have unignorable effects toward the effectiveness of the computational fragment linking described in this paper. Fragment growth and fragment merge would be alternative methodologies for novel compounds generation using the model 5CGD. Based on the identified fragment hits, linkers and functional groups can be introduced to improve the chemical physical properties and drug likability. These works may beyond the scope of this paper, and 4OO9 was focused to illustrate the study approach.

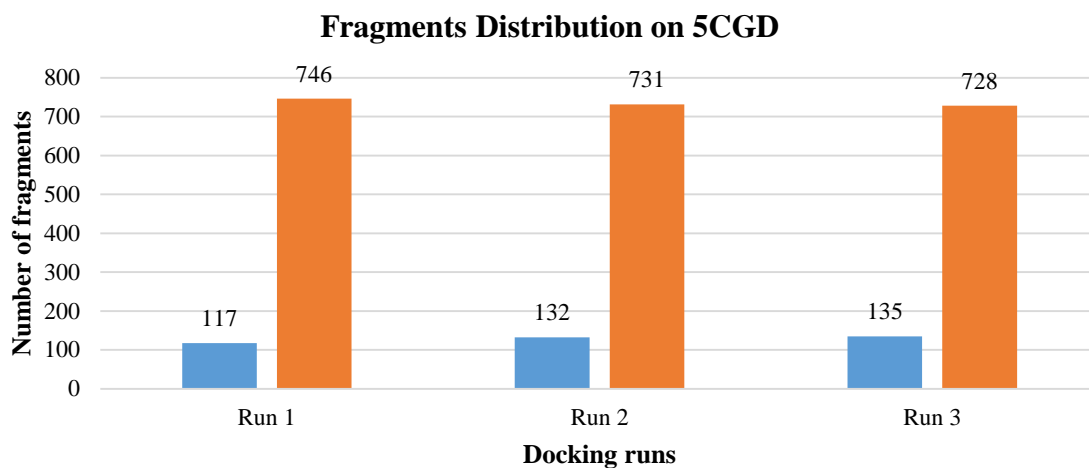


**Figure 16.** Fragments sorting based on 5CGD

The distribution of fragments towards the upper and bottom region of 5CGD. Blue bars represent the number of fragments in the upper region. Orange bars represent the number of fragments in the bottom region.

## 4.0 DISCUSSION

In order to further validate our *in silico* synthesized compounds, we tried to find out whether there are existing mGlu<sub>5</sub> allosteric modulators that are structurally similar to our *in silico* synthesized compounds.

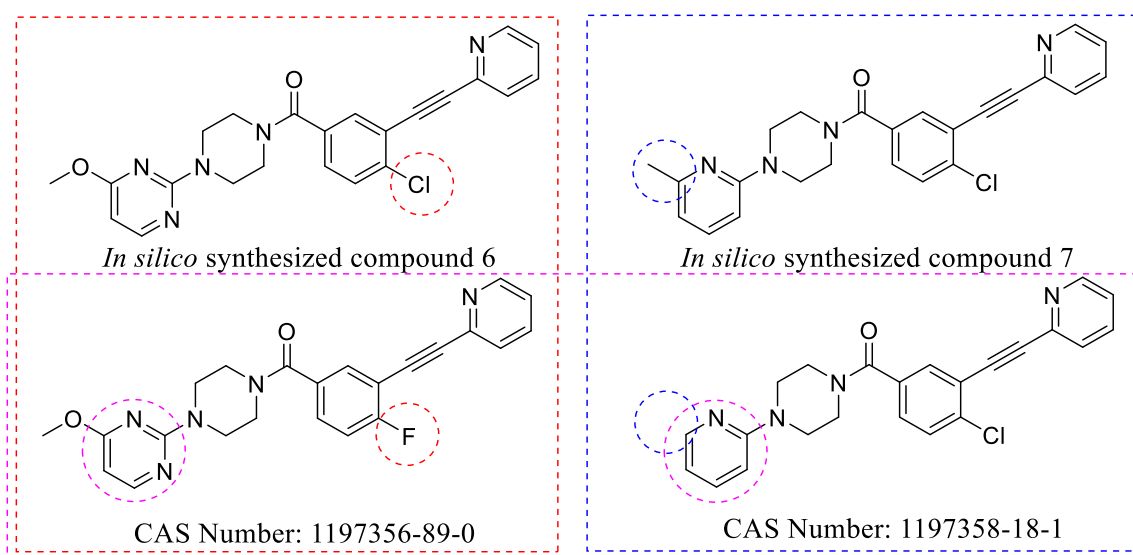
A similarity search was performed on SciFinder (scifinder.cas.org) using compound 1, which is the most potent one according to our prediction, as listed on **Table 3**. The search was started with chemical structures and the search type was similarity. The hits with tanimoto coefficients over 85% were selected for further analysis. Interestingly, we identified one compound (CAS Number: 1197356-89-0), which is 90% similar towards compound 1, to be



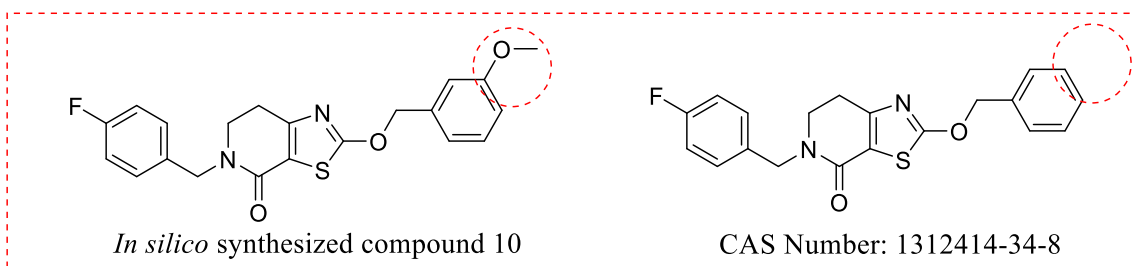
almost identical towards compound 6 (97%) listed on **Table 3**. The only difference between 1197356-89-0 and compound 6 is the substitution on the benzene ring (**Fig. 17A**), with compounds 6 featuring chlorine substitution instead of a fluorine. 1197356-89-0 is a compound that first published on a US patent, *Piperazine Metabotropic Glutamate Receptor Negative Allosteric Modulators for Anxiety/Depression*, US 2009/0325964 A1. A competitive binding assay, that assesses compounds' ability to displace MPEP from Hek-293 cell membrane expressing rat mGlu<sub>5</sub> receptors, was used to identify the compounds' activity in that patent(67). Median  $K_i$  value for 1197356-89-0 is 20 nM ( $\text{Log}K_i = 1.30$ ), while our prediction for compound 6 is 324.2 nM ( $\text{Log}K_i = 2.51$ ). Since logarithmic transformation was used in our QSAR model simulation, the difference in absolute  $K_i$  value is reasonable and acceptable. The promising biological activity of 1197356-89-0 demonstrates that our method for *in silico* design can identify promising chemotypes for targets of interest when an existing crystal structure is available to build a model around. We further assessed whether the difference between the chlorine and fluorine would be the key component for the activity. It is known that fluorine could function as a hydrogen bond acceptor to intermediate receptor-ligand interactions. But for chlorine, there is almost no reported role in hydrogen bond interactions. 1197358-18-1, which is another compound in that patent, has chlorine connected towards the benzene ring (**Fig. 17A**). The major difference between 1197358-18-1 and 1197356-89-0 is the substitution on the piperazine ring. For 1197358-18-1, a pyridine is attached, while for 1197356-89-0, a pyrimidine is attached. Median  $K_i$  value for 1197358-18-1 is 3 nM ( $\text{Log}K_i = 0.48$ ), which shows that the change from fluorine to chlorine does not decrease the allosteric regulation potency. Among our *in silico* synthesized compounds, with an additional methyl group on pyridine, compound 7 listed on **Table 3** shares 96% similarity towards 1197358-18-1 (**Fig. 17A**). The predicted  $K_i$  value for compound 7 is 545.0 nM ( $\text{Log}K_i = 2.73$ ). So, the

potency of 1197358-18-1 turns out to be another evidence to support our *in silico* design. And the consistency between predicted  $K_i$  value and experimental data shows our evaluation is reliable to some extent. Through searching the original allosteric modulator database, which used for our fragments generation, there are no identical structures to these two compounds in patent. Although similar compounds do exist, but they share a low tanimoto coefficient.

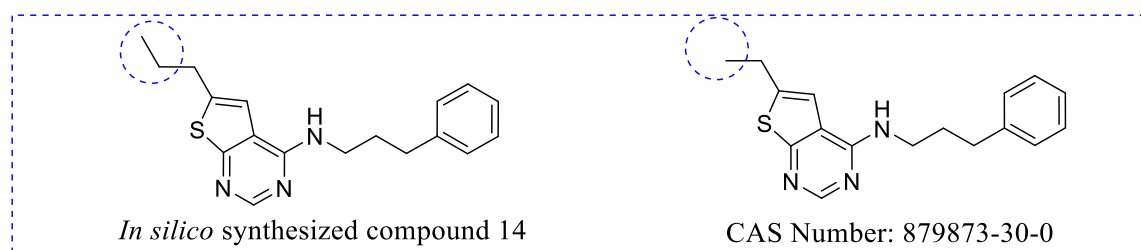
**A**



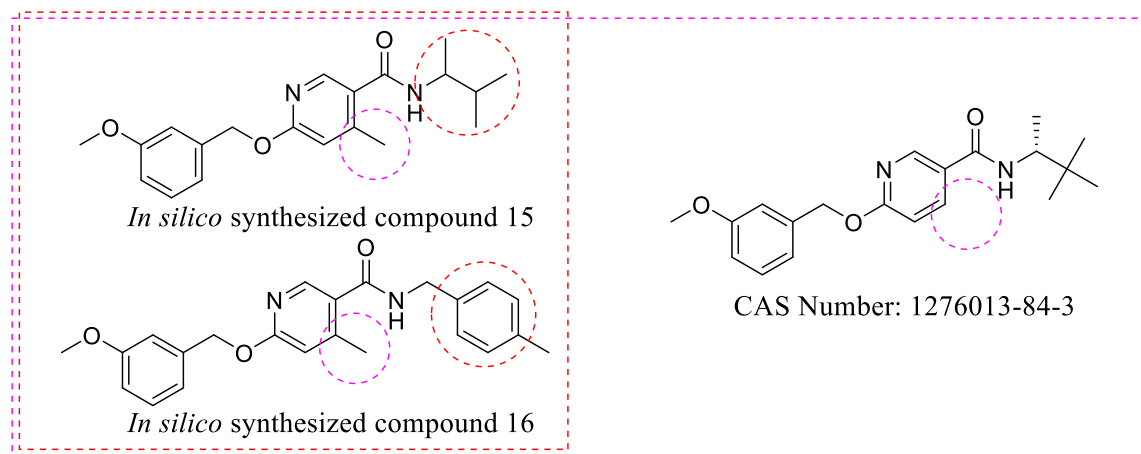
**B**



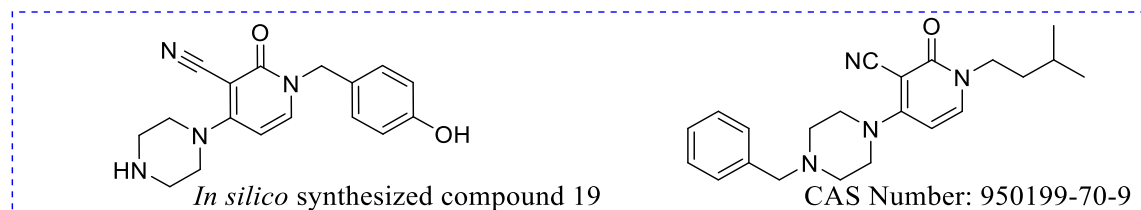
**C**



**D**



**E**



**F**

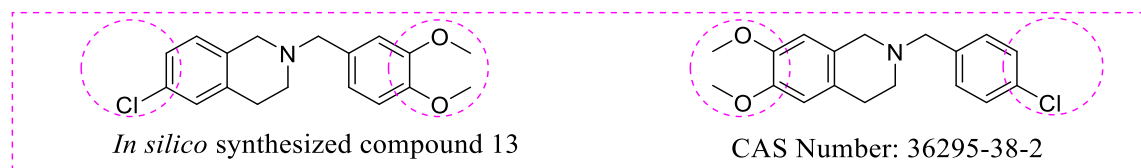


**Figure 17.** Structural comparison between *in silico* synthesized compounds and existing compounds with known mGluR allosteric activities.

Comparisons were circled with dashed lines in red, blue, and pink colors. The major difference inside each group was circled with the same color as their group. The CAS number for patented

compounds and the corresponding number for *in silico* synthesized compounds are listed under each structure.

Meanwhile, since compounds 10, 13-16, and 18 have distinctive structures to 1,2-diphenylethyne analogs and piperazine scaffold described in the above mentioned patent, similarity searches for them on Scifinder were continued. 1312414-34-8, which shares 93% similarity with compound 10, is a compound that published on a US patent, *Bicyclic Thiazoles as Allosteric Modulators of Mglur5 Receptors*, US 2012/0258955 A1.(68) 1312414-34-8 was tested with functional assay, and the pEC<sub>50</sub> value is 5.29. Compound 10 has one additional methoxy group connected with the aromatic ring, when compared with 1312414-34-8 (**Fig. 17B**). 879873-30-0 is a compound that included on a US patent, *Novel Thieno-Pyridine and Thieno-Pyrimidine Derivatives and Their Use as Positive Allosteric Modulators of Mglur2-Receptors*, US 20070275984 A1.(69) 879873-30-0 shares 97% similarity towards compound 14. Compound 14 has one additional methyl group connected with alkane chain (**Fig. 17C**). [<sup>35</sup>S]GTP<sub>γ</sub>S binding assay was performed to assess the allosteric activities. 879873-30-0 left-ward shifts the agonist mGlu<sub>2</sub> concentration-response curve by 2-3.5 folds. Compounds 15/16 share same O-benzyl nicotinamide scaffold. The difference is the aromatic or alkane substitution connected to the peptide bond. 1276013-84-3, which shares 92% similarity with compound 15, is published on a US patent, *O-benzyl Nicotinamide Analogs as Mglur5 Positive Allosteric Modulators*, US 2011/0183980 A1 (**Fig. 17D**). (70) The EC<sub>50</sub> (nM) for 1276013-84-3 recorded on the patent is 120. Compound 19 shares same 3-cyano-pyridone scaffold with 950199-70-9 with an 83% similarity (**Fig. 17E**). 950199-70-9 is listed on the a US patent, *1, 4-Disubstituted 3-Cyano-Pyridone Derivatives and Their Use As Positive Allosteric Modulators of MGLUR2-Receptors*, US 2014/0315903 A1.(71) The pEC<sub>50</sub> of 950199-70-9 for the GTP<sub>γ</sub>S-PAM is 6.7. For compound 13,

it shares 83% similarity with 36295-38-2 (**Fig. 17F**). Dr. Rosaria Gitto's group reported that *N*-substituted isoquinoline derivatives could be functioned as potential AChE inhibitors. But, there is no reported activities on metabotropic glutamate receptors for *N*-substituted isoquinoline derivatives, as 36295-38-2.

The recall of compounds with existing scaffolds and reported effects on mGluR shown that the approach we generated is feasible. And the discovery of compounds with unreported activities on mGluR revealed that our approach is doable for exploring and designing novel compounds.

## 5.0 CONCLUSION

In this study, we demonstrated a case study of designing allosteric modulators on metabotropic glutamate receptor 5 using *in silico* fragment-based novel compounds design. A GPCR allosteric modulator specific fragment library was generated, which could be used for future studies. Various computational methodologies, including benchmarking dataset validation, docking studies, QuaSAR model simulation, etc. were used to construct the *in silico* compounds and validate the effectiveness of this lead generation strategy. The effects associated with the rotation of toggle switch, Trp785, were considered and evaluated. The dramatic conformational changes on critical residues would have unignorable effects toward the effectiveness of the computational methodology described in this paper. The determination of using one model or combining two or more models should be specified at the beginning of the study design. Among the top 20 *in silico* synthesized compounds, as listed in **Table 2**, diversified structures could be observed. Through the compound similarity search on the Scifinder, multiple patents were identified to contain

compounds that have similar structural features with our *in silico* design. Series of compounds with reported mGluR allosteric activities were recurred in this case study for designing mGlu<sub>5</sub> allosteric modulators. The *in silico* designed compounds with reported scaffolds may fill SAR holes in the known, patented series of mGlu<sub>5</sub> modulators. And the recall of compounds with existing scaffolds and reported effects on mGluR shown that the approach we generated is feasible. Meanwhile, the generation of compounds without reported activities on mGluR indicates that our approach is doable for exploring and designing novel compounds. The medicinal chemistry synthesis for these *in silico* compounds is in progress in our laboratory, and we will perform the experiments to confirm our predictions in the future to find out whether they (1) are mGlu<sub>5</sub> allosteric modulators, (2) retain the ranking order the same way as our prediction, (3) have better activities than known modulators or not in a head-to-head comparison. Our case study on designing allosteric modulators on mGlu<sub>5</sub> suggested that this computational fragment-based approach is a reliable and powerful methodology for facilitating the future compounds design processes.

## **6.0 FUTURE PROSPECTIVE**

### **6.1 METABOTROPIC GLUTAMATE RECEPTOR 5 ALLOSTERIC REGULATION**

In the current study, 20 *in silico* synthesized compounds were designed and predicted to be potential allosteric modulators on mGlu<sub>5</sub>. Computational simulation and prediction do provide evidences for validating the results, but the neglect of experimental verification may lose the confidence for the effectiveness of this established computational approach. To further validate

the allosteric activity of the in silico synthesized compounds, [35S]GTP $\gamma$ S binding assay would be conducted. In this assay, upon activation of the GPCR, the receptor changes conformation exposing a binding site for a G-protein complex. Once this G-protein complex is bound, the G $\alpha$  protein can release GDP and bind GTP. Allosteric modulators would have influences on orthosteric activities, which would consequently affect the amount of GDP released and GTP bound.

The development of bitopic compounds is another attractive area of research. Combining the high affinity, through orthosteric regulation, and the high selectivity, through allosteric regulation, bitopic compounds would possess promising biological properties. Linkers could be designed and introduced between mGlu<sub>5</sub> orthosteric ligands and allosteric modulators. Computational methodologies and biological assays could be combined to verify the activity. Further modifications could be continued to increase the affinity and efficacy of newly designed compounds. Although for class C GPCRs the orthosteric site and allosteric site are usually distant from each other, the design of bitopic ligands is a meaningful attempt for adopting a novel strategy of compounds design.

## **6.2 CANNABINOID RECEPTOR 2 ALLOSTERIC REGULATION**

The case study of designing allosteric modulators on mGlu<sub>5</sub> provided the confidence, to some extent, that the computational fragment-based approach is a novel and productive strategy for generating modulators and studying GPCRs' allosteric regulation. There are two types of cannabinoid receptors, type 1 and type 2. Cannabinoid receptor 1 (CB1) is mainly distributed in the brain and central nervous system, while cannabinoid receptor 2 (CB2) is mostly located in the

peripheral organs. CB2 is a vital target for treating autoimmune, osteoporosis, immune system cancer, and drug abuse. Designing CB2 allosteric modulators would be an alternative and considerable approach in this field of research.

A CB2 homology model has been constructed based on the crystalized structure of CB1 (PDB entry: 5TGZ) which is recently reported in 2016 from Zhi-Jie Liu's group. The orthosteric and allosteric binding pocket on CB2 were predicted and verified with reported CB2 selective ligands and modulators. With the established computational fragment-based approach, novel CB2 allosteric modulators could be designed and tested. Biological assays, to be specific, [<sup>35</sup>S]GTPγS binding assay would be conducted to validate the predicted allosteric activities. Furthermore, the development of CB2 selective bitopic ligands can be followed. Considering that cannabinoid receptors are belonging to class A GPCRs that have their orthosteric and allosteric pockets adjacent and both located in the transmembrane domain, developing bitopic ligands is promising.

## 7.0 APPENDIX

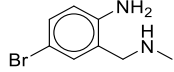
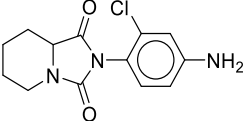
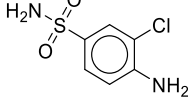
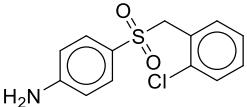
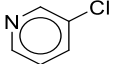
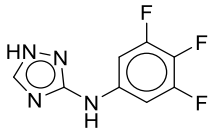
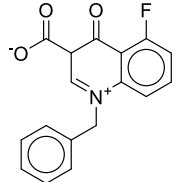
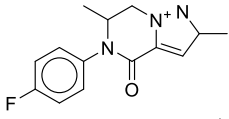
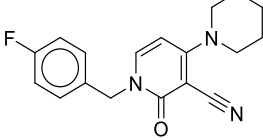
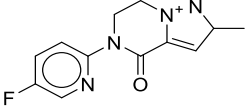
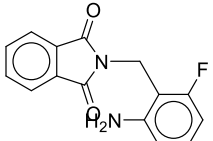
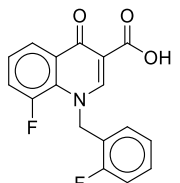
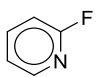
### 7.1 120 HIGHEST SCORED FRAGMENTS IN THE UPPER REGION

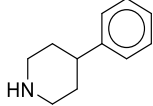
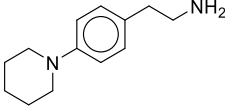
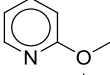
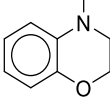
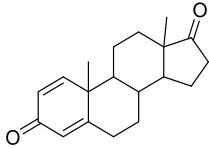
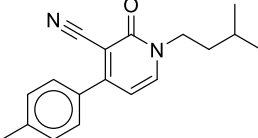
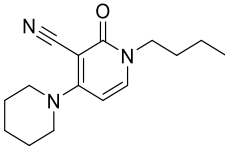
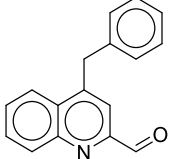
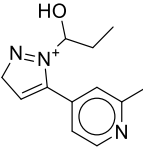
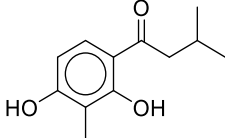
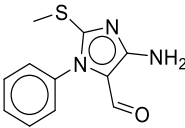
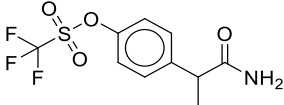
Structure, frequency, molecular weight, logP (o/w), number of hydrogen bond acceptors, and number of hydrogen bond donors of 120 highest scored fragments in the upper region are summarized in **Supplementary Table 1**.

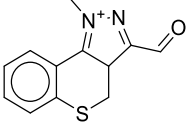
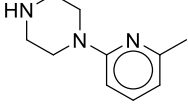
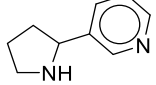
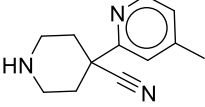
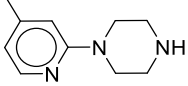
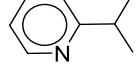
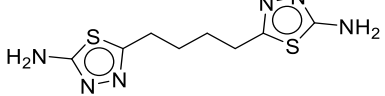
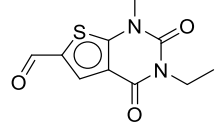
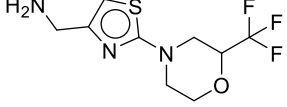
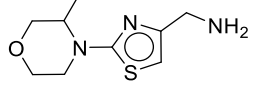
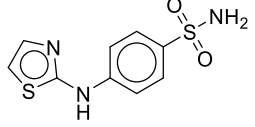
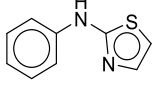
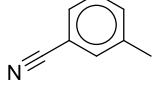
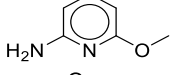
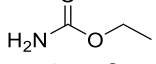
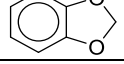
**Supplementary table 1.** 120 highest scored fragments in the upper region

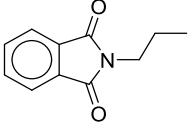
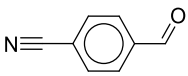
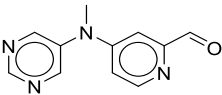
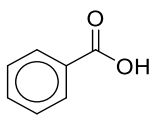
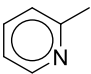
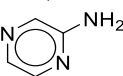
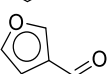
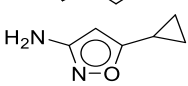
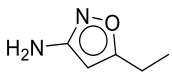
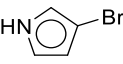
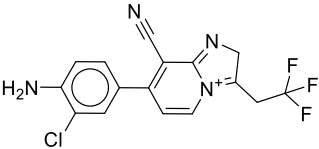
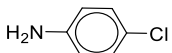
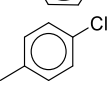
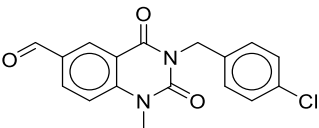
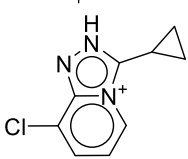
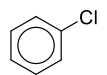
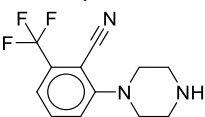
No.	Structure	Frequency	LogP(o/w)	M.W.	Hydrogen bond donor	Hydrogen bond acceptor
-----	-----------	-----------	-----------	------	---------------------	------------------------



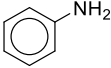
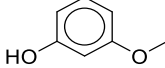
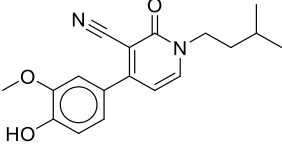
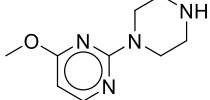
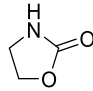
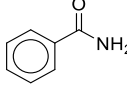
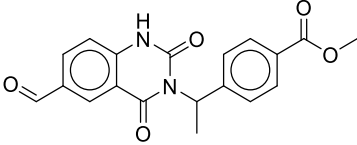
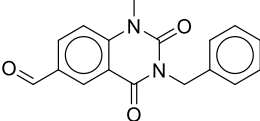
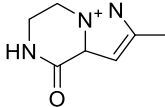
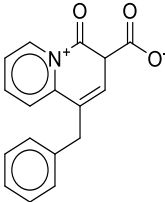
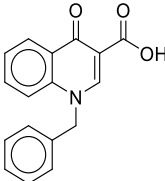
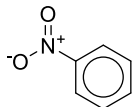
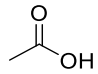
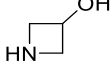
1		6	1.85	215.09	2	1
2		6	1.78	279.73	1	2
3		6	0.29	206.65	2	2
4		6	2.81	281.76	1	2
5		6	1.27	113.55	0	1
6		6	1.50	214.15	3	3
7		6	2.76	297.29	0	1
8		6	1.91	260.29	0	2
9		6	2.51	311.36	0	2
10		6	0.62	247.25	0	3
11		6	2.34	270.26	1	2
12		6	3.08	315.27	2	3
13		6	1.23	97.09	0	1

14		6	2.16	161.25	1	1
15		6	2.14	204.32	1	1
16		6	1.04	109.13	0	1
17		6	1.42	149.19	0	1
18		6	3.26	284.40	0	2
19		6	3.43	280.37	0	2
20		6	1.97	259.35	0	2
21		6	4.08	247.30	0	2
22		6	1.52	218.28	1	3
23		6	2.71	208.26	2	3
24		6	2.26	233.30	1	2
25		6	2.09	297.25	1	4

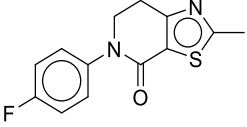
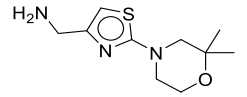
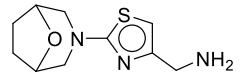
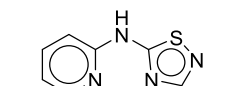
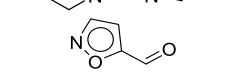
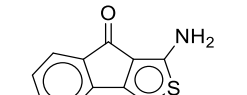
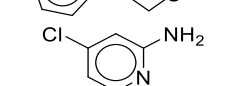
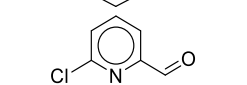
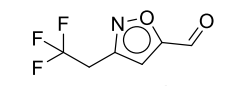
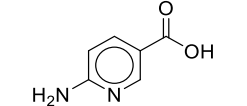
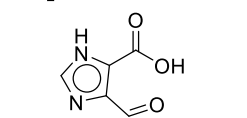
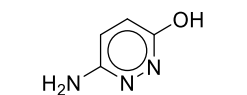
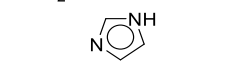
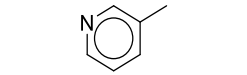
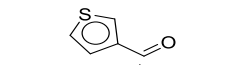
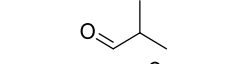
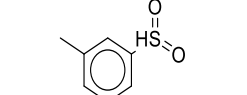
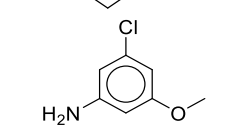
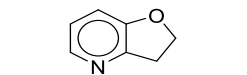
26		6	1.90	231.30	0	2
27		6	0.51	177.25	1	2
28		6	1.11	148.21	1	2
29		6	1.21	201.27	1	3
30		6	0.59	177.25	1	2
31		6	2.29	121.18	0	1
32		6	1.81	256.36	2	4
33		6	0.95	238.27	0	3
34		6	0.47	267.27	1	3
35		6	0.05	213.30	1	3
36		6	0.70	255.32	2	3
37		6	2.27	176.24	1	1
38		6	1.90	117.15	0	1
39		6	0.77	124.14	1	1
40		6	-0.19	89.09	1	1
41		6	1.57	122.12	0	2

42		6	2.03	189.21	0	2
43		6	1.49	131.13	0	2
44		6	-0.06	214.23	0	4
45		6	1.58	122.12	2	2
46		6	1.10	93.13	0	1
47		6	-0.63	95.10	1	2
48		6	0.67	96.08	0	1
49		6	0.53	124.14	1	1
50		6	0.66	112.13	1	1
51		5	1.47	145.99	1	0
52		5	3.01	351.74	1	2
53		5	1.83	127.57	1	0
54		5	2.80	126.59	0	0
55		5	3.25	328.76	0	3
56		5	2.85	194.64	0	1
57		5	2.50	112.56	0	0
58		5	1.67	255.24	1	2

59		5	3.55	373.34	0	4
60		5	1.89	299.26	2	5
61		5	2.09	312.30	1	1
62		5	0.77	194.21	2	2
63		5	1.35	125.15	1	1
64		5	2.85	312.30	0	3
65		5	4.88	242.22	0	1
66		5	1.91	260.29	0	2
67		5	4.69	224.23	0	1
68		5	3.42	225.22	0	2
69		5	4.69	224.23	0	1
70		5	1.23	97.09	0	1
71		5	0.38	55.08	0	1
72		5	1.53	107.16	1	0

73		5	1.23	93.13	1	0
74		5	1.59	124.14	1	2
75		5	2.81	312.37	1	4
76		5	-0.57	194.24	1	3
77		5	-0.52	87.08	1	1
78		5	0.85	121.14	1	1
79		5	2.86	352.35	1	4
80		5	2.66	294.31	0	3
81		5	-0.77	152.18	1	2
82		5	2.66	279.29	0	1
83		5	2.78	279.29	2	3
84		5	1.84	123.11	0	0
85		5	-0.08	60.05	2	2
86		5	-1.03	73.10	2	2

87		5	2.63	323.38	1	3
88		5	0.56	234.24	3	4
89		5	0.93	109.13	2	1
90		5	1.90	108.14	1	1
91		5	0.33	310.36	2	4
92		5	1.27	138.12	3	3
93		5	0.23	120.16	1	2
94		5	-0.09	188.23	1	3
95		5	-0.09	188.23	1	3
96		5	1.03	126.16	1	1
97		5	1.67	156.25	1	1
98		5	2.95	257.36	0	2
99		5	0.95	238.27	0	3
100		5	2.20	286.31	1	3

101		5	1.90	262.31	0	2
102		5	0.45	227.33	1	3
103		5	0.36	225.32	1	3
104		5	1.02	178.22	1	3
105		5	0.04	97.07	0	2
106		5	2.60	201.25	1	1
107		5	1.04	128.56	1	1
108		5	1.56	141.56	0	2
109		5	1.06	179.10	0	2
110		5	0.08	138.13	3	3
111		5	-1.00	140.10	4	5
112		5	0.74	111.10	2	3
113		5	-0.52	68.08	2	2
114		5	1.14	93.13	0	1
115		5	1.48	112.15	0	1
116		5	1.02	72.11	0	1
117		5	1.46	156.21	0	2
118		5	1.89	157.60	1	1
119		5	0.50	121.14	0	2

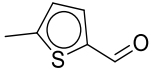
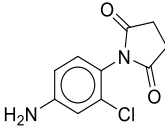
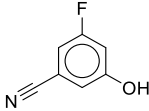
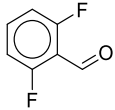
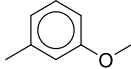
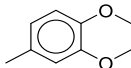
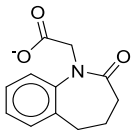
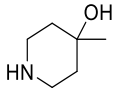


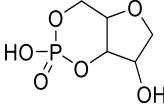
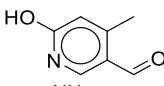
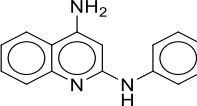
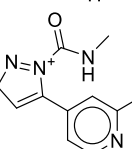
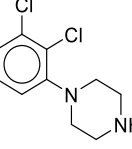
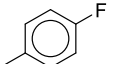
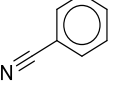
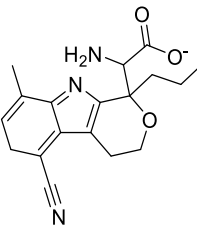
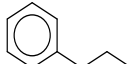
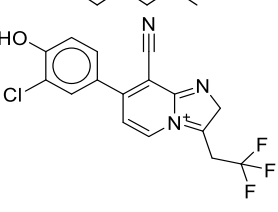
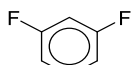
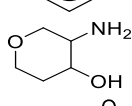
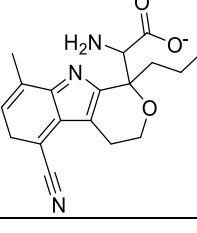
120		5	0.40	74.08	2	2
-----	---	---	------	-------	---	---

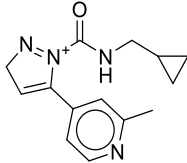
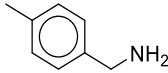
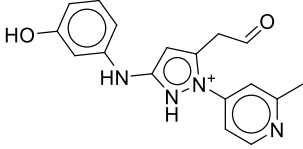
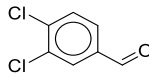
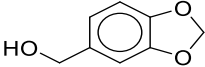
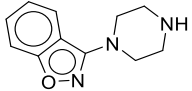
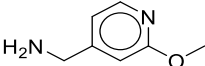
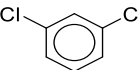
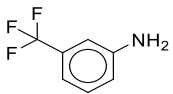
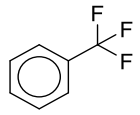
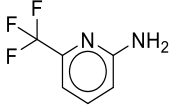
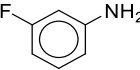
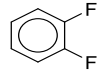
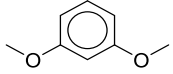
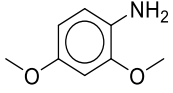
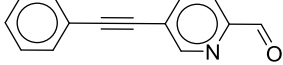
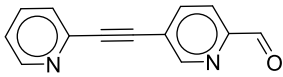
## 7.2 80 HIGHEST SCORED FRAGMENT IN THE BOTTOM REGION

Structure, frequency, molecular weight, logP (o/w), number of hydrogen bond acceptors, and number of hydrogen bond donors of 80 highest scored fragments in the bottom region are summarized in **Supplementary Table 2**.

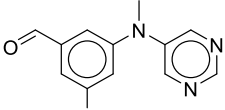
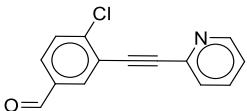
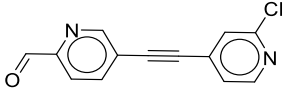
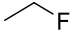
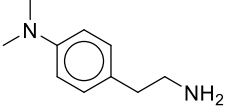
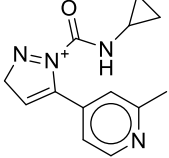
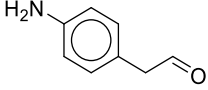
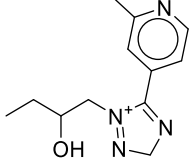
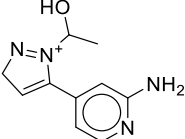
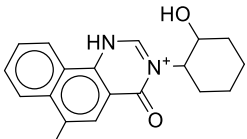
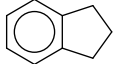
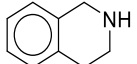
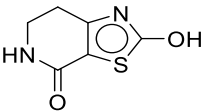
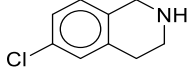
**Supplementary table 2.** 80 highest scored fragments in the bottom region

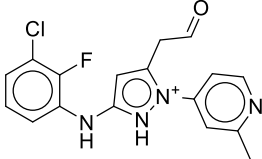
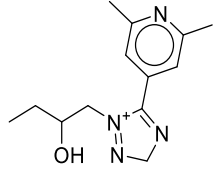
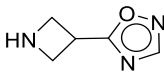
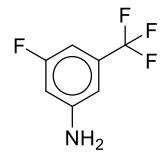
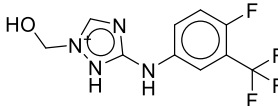
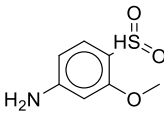
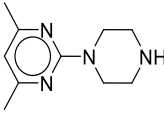
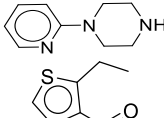
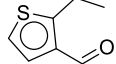
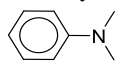
No.	Structure	Frequency	LogP(o/w)	M.W.	Hydrogen bond donor	Hydrogen bond acceptor
1		6	1.54	126.18	0	1
2		6	0.90	224.65	1	2
3		6	1.52	137.11	1	2
4		6	2.14	142.10	0	1
5		6	2.20	122.17	0	1
6		6	1.90	152.19	0	2
7		6	1.33	218.23	0	1
8		6	0.26	115.18	2	2

9		6	-1.97	196.10	3	6
10		6	1.03	137.14	1	3
11		6	3.26	235.29	2	1
12		6	1.00	217.25	1	3
13		6	2.26	231.13	1	1
14		6	2.36	110.13	0	0
15		6	1.57	103.12	0	1
16		6	0.88	326.38	1	4
17		6	3.63	120.20	0	0
18		6	3.37	352.72	1	3
19		6	2.25	114.09	0	0
20		6	-1.07	117.15	2	3
21		6	0.88	326.38	1	4

22		6	1.82	257.32	1	3
23		6	1.46	121.18	1	1
24		6	2.33	309.35	1	3
25		6	3.05	175.01	0	1
26		6	1.09	152.15	1	3
27		6	1.24	203.25	1	2
28		6	0.33	138.17	1	2
29		5	3.13	147.00	0	0
30		5	2.21	161.13	1	0
31		5	2.84	146.11	0	0
32		5	1.30	162.11	1	1
33		5	1.42	111.12	1	0
34		5	2.21	114.09	0	0
35		5	1.86	138.17	0	2
36		5	1.18	153.18	1	2
37		5	3.27	207.23	0	2
38		5	2.00	208.22	0	3



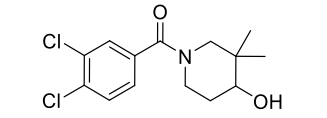
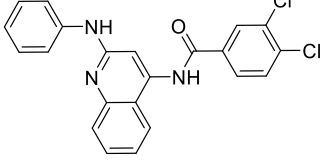
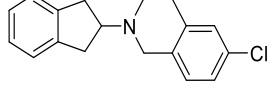
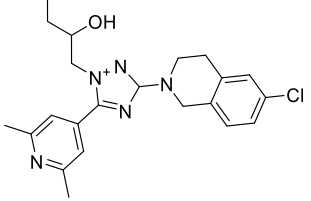
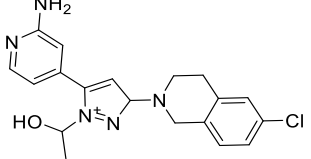
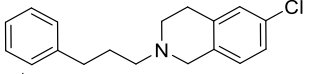
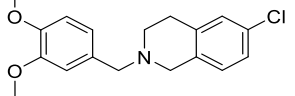
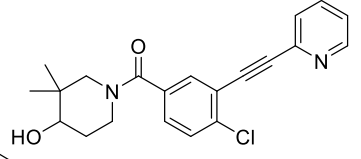
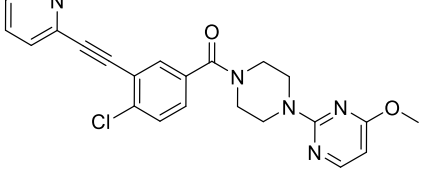
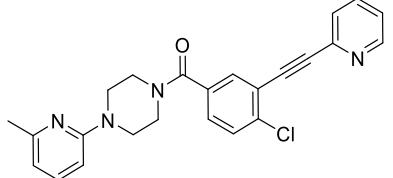
57		5	1.87	247.69	0	3
58		5	3.90	241.68	0	2
59		5	3.07	242.66	0	3
60		5	0.75	48.06	0	0
61		5	1.17	164.25	1	1
62		5	1.65	243.29	1	3
63		5	1.25	135.17	1	1
64		5	0.69	233.30	1	4
65		5	0.38	205.24	2	3
66		5	4.28	309.39	1	2
67		5	3.03	118.18	0	0
68		5	1.59	133.19	1	1
69		5	-0.38	170.19	2	3
70		5	2.22	167.64	1	1

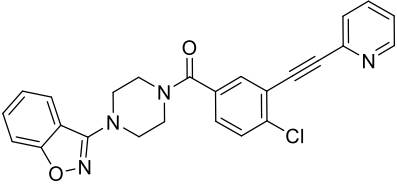
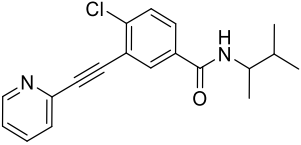
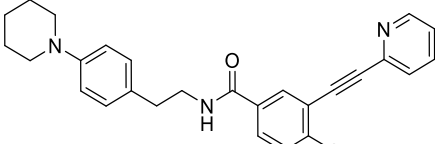
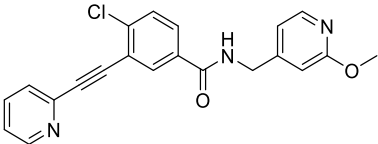
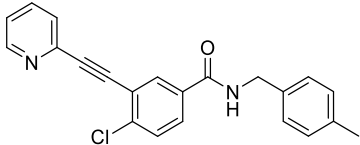
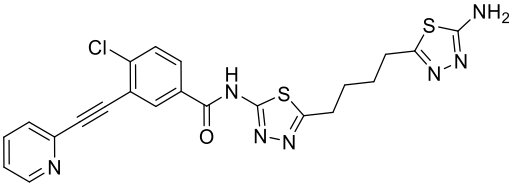
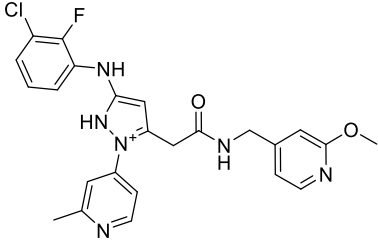
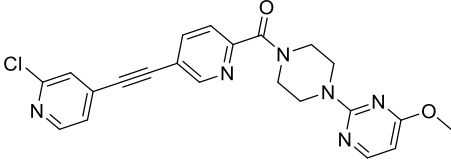
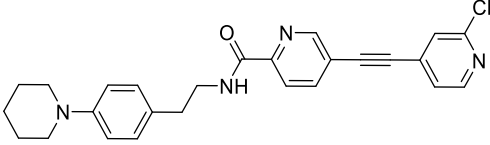
71		5	3.34	345.79	0	2
72		5	0.99	247.32	1	4
73		5	-1.31	125.13	1	3
74		5	2.43	179.12	1	0
75		5	1.26	277.20	3	3
76		5	0.45	187.22	1	2
77		5	-0.38	192.27	1	3
78		5	0.25	163.22	1	2
79		5	2.13	140.21	0	1
80		5	1.82	121.18	0	0

### 7.3 124 *IN SILICO* SYNTHESIZED COMPOUNDS WITH DOCKING SCORE OVER 7

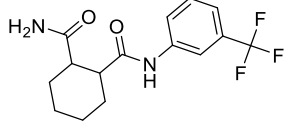
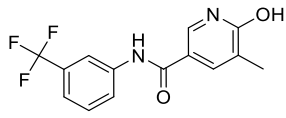
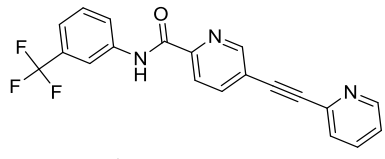
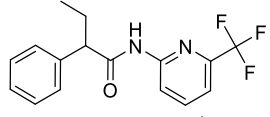
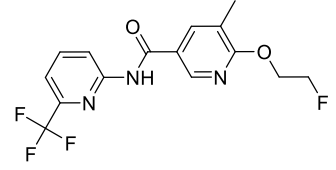
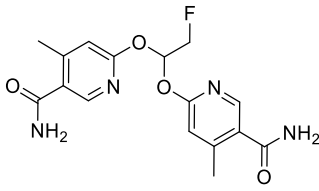
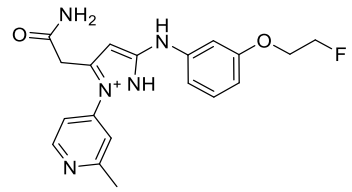
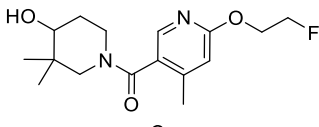
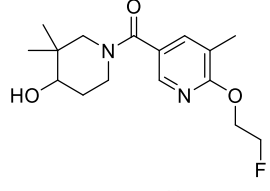
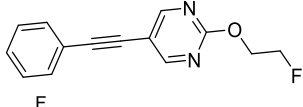
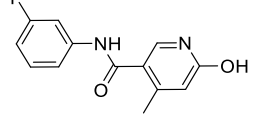
Structure, molecular weight, logP (o/w), number of hydrogen bond acceptors, and number of hydrogen bond donors of 124 *in silico* synthesized compounds with docking score over 7 are summarized in **Supplementary Table 3**.

**Supplementary table 3.** 124 *in silico* synthesized compounds with docking score over 7

No.	Structure	M.W.	LogP(o/w)	H-bond acceptor	H-bond Donor
1		302.20	3.34	2	1
2		408.29	6.10	2	2
3		283.80	4.39	1	0
4		412.94	3.47	5	1
5		370.86	2.77	4	2
6		285.82	4.81	1	0
7		317.82	3.98	3	0
8		368.86	4.18	3	1
9		433.90	2.99	4	0
10		416.91	4.07	3	0

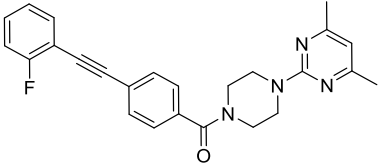
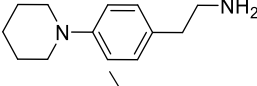
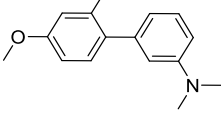
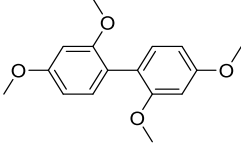
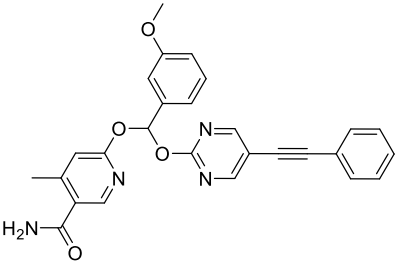
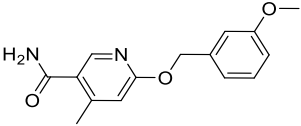
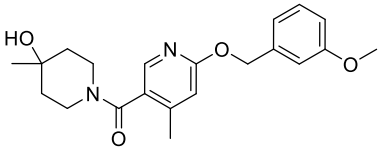
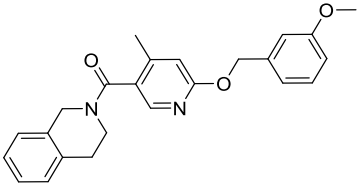
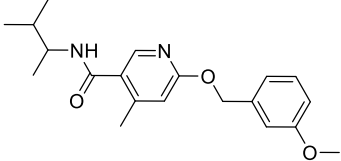
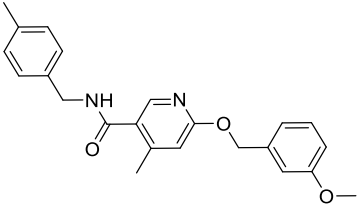
11		442.91	4.81	3	0
12		326.83	5.04	2	1
13		443.98	6.03	2	1
14		377.83	4.22	3	1
15		360.84	5.35	2	1
16		496.02	5.49	6	2
17		481.94	3.67	3	1
18		434.89	2.17	5	0
19		444.97	5.21	3	1

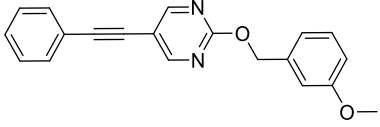
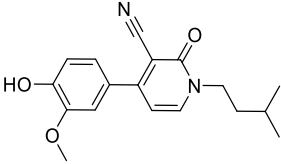
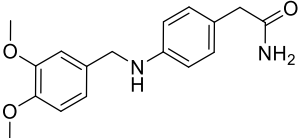
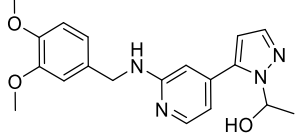
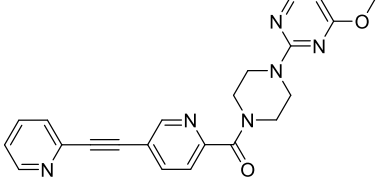
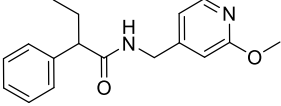
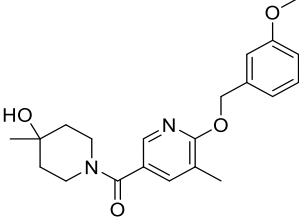
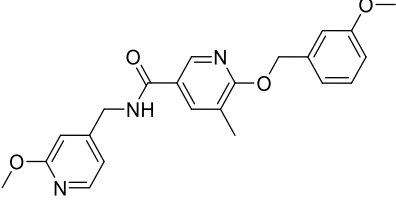
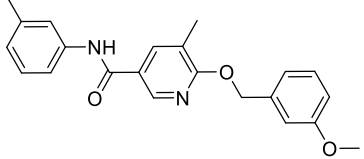
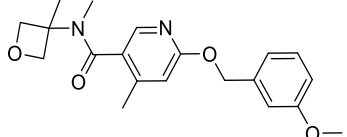


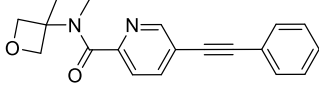
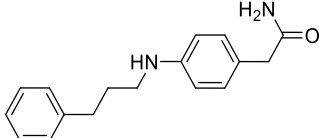
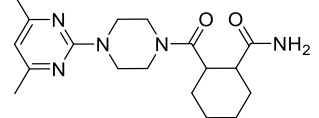
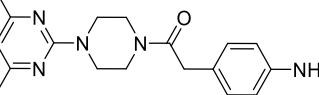
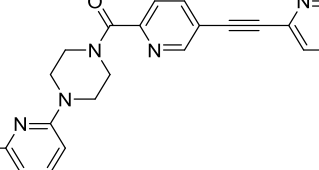
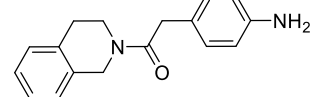
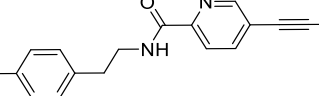
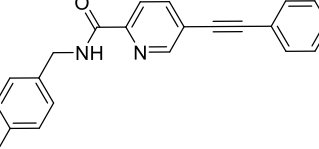
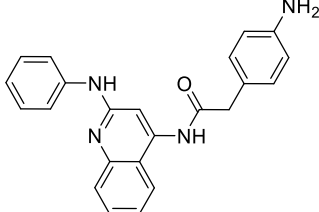
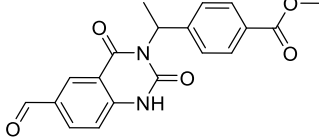
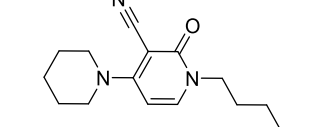
20		314.31	2.12	2	2
21		296.25	3.03	3	2
22		367.33	3.99	3	1
23		308.30	3.83	2	1
24		343.28	2.50	3	1
25		348.33	0.64	4	2
26		370.41	1.72	3	1
27		310.37	1.69	3	1
28		310.37	1.69	3	1
29		242.25	2.67	2	0
30		246.24	2.25	3	2

31		366.39	4.29	3	1
32		382.34	3.04	3	3
33		297.29	5.07	0	1
34		329.29	4.24	2	1
35		333.29	2.12	4	1
36		257.26	3.57	3	0
37		434.45	3.98	3	0
38		242.22	4.88	1	0
39		260.29	1.91	2	0
40		396.37	3.20	3	3

41		369.30	2.98	4	4
42		423.39	2.81	5	4
43		417.44	2.52	4	0
44		427.52	5.56	2	1
45		311.36	2.51	2	0
46		247.25	0.62	3	0
47		441.45	2.54	5	0
48		255.26	1.83	2	1
49		304.34	3.30	1	1
50		375.38	5.18	2	2
51		416.46	3.79	3	0

52		414.48	3.98	3	0
53		204.32	2.14	1	1
54		257.33	3.77	2	0
55		274.32	3.76	4	0
56		466.50	4.56	5	1
57		272.30	2.09	3	1
58		370.45	3.01	4	1
59		388.47	4.34	3	0
60		342.44	4.22	3	1
61		376.46	4.53	3	1

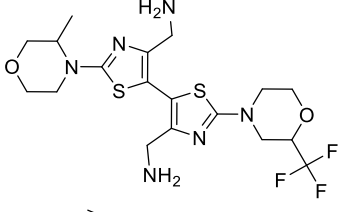
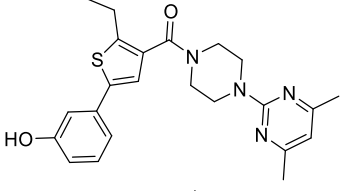
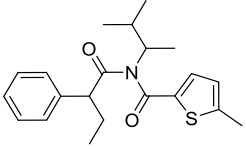
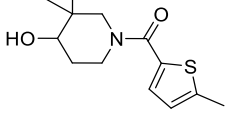
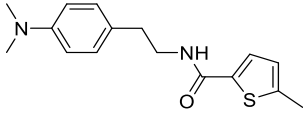
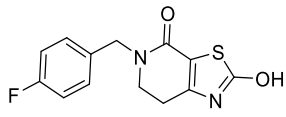
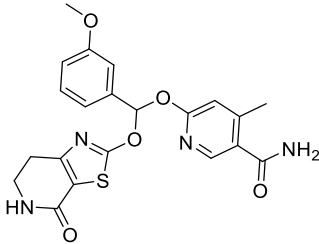
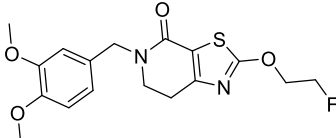
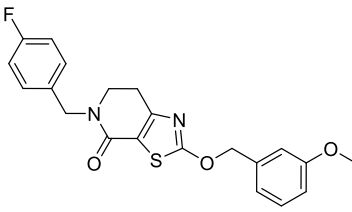
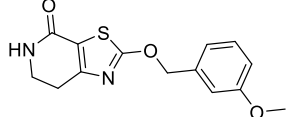
62		316.36	4.34	3	0
63		312.37	2.81	4	1
64		300.36	2.07	3	2
65		355.42	2.18	5	2
66		400.44	1.10	5	0
67		284.36	3.06	2	1
68		370.45	3.01	4	1
69		393.44	3.40	4	1
70		362.43	4.44	3	1
71		356.42	2.74	4	0

72		306.36	2.93	3	0
73		268.36	2.90	1	2
74		345.45	-0.58	4	1
75		325.42	0.54	3	1
76		383.45	2.18	4	0
77		266.34	2.51	1	1
78		410.52	4.13	3	1
79		326.40	4.72	2	1
80		368.44	4.30	2	3
81		352.35	2.86	4	1
82		259.35	1.97	2	0

83		395.49	1.57	5	3
84		321.40	2.60	3	2
85		248.33	1.18	2	2
86		261.36	2.43	2	1
87		320.39	2.96	3	1
88		305.33	3.66	3	2
89		471.58	3.49	3	2
90		309.35	2.33	3	1
91		310.36	0.33	4	2

92		432.52	3.44	4	2
93		359.35	0.91	4	4
94		402.43	0.49	5	2
95		454.43	1.73	4	1
96		435.46	-1.39	6	3
97		362.45	2.44	4	3
98		235.29	3.26	1	2
99		237.30	1.01	2	1
100		300.36	0.02	3	0
101		241.29	1.99	1	0
102		336.39	2.16	2	1



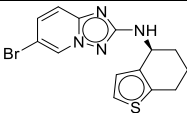
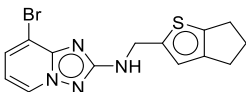
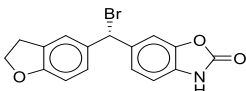
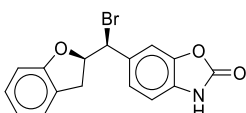
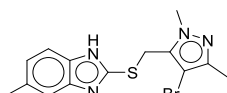
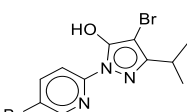
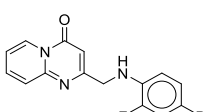
103		478.56	0.32	6	2
104		422.55	3.03	4	1
105		357.52	5.42	2	0
106		253.37	1.83	2	1
107		288.42	2.70	1	1
108		278.31	1.76	3	1
109		440.48	1.89	5	2
110		366.41	1.69	4	0
111		398.46	3.81	3	0
112		290.34	1.67	3	1

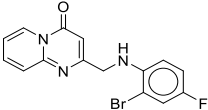
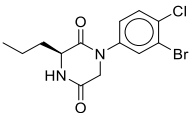
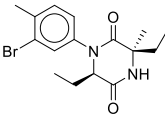
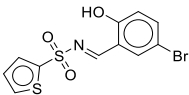
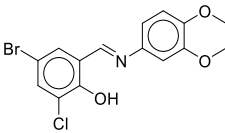
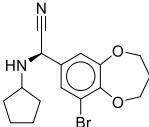
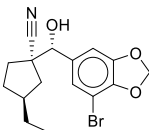
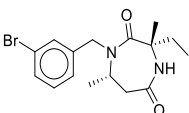
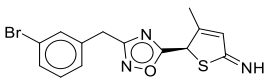
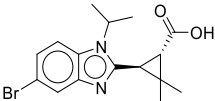
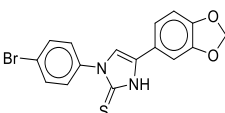
113		396.50	2.29	5	3
114		311.45	4.33	2	1
115		343.45	3.49	4	1
116		227.33	0.45	3	1
117		433.54	2.45	5	1
118		473.48	2.46	5	1
119		225.32	0.36	3	1
120		330.46	1.43	3	0
121		341.44	3.05	2	0
122		302.44	3.30	1	1
123		276.36	2.46	2	1
124		300.30	3.23	2	1

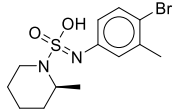
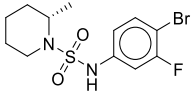
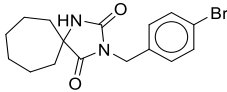
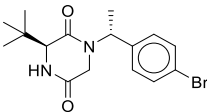
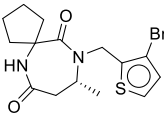
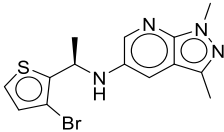
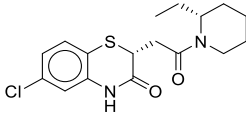
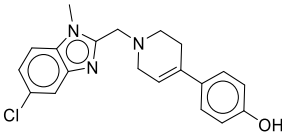
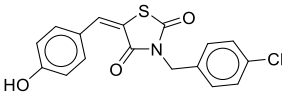
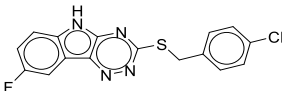
## 7.4 DECOYS INVOLVED IN THE ENRICHMENT TEST

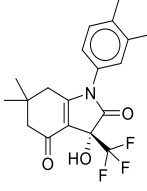
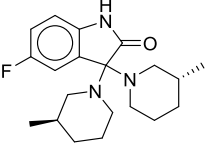
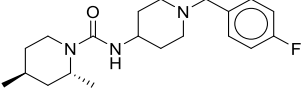
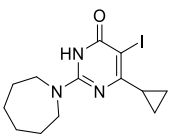
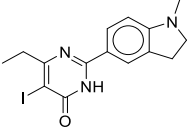
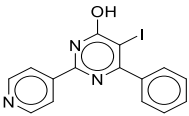
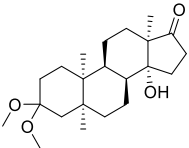
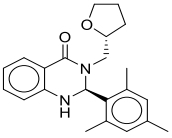
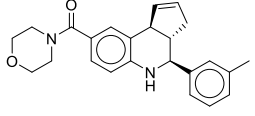
Structure, molecular weight, logP (o/w), number of hydrogen bond acceptors, number of hydrogen bond donors, and number of rotatable bonds of decoys are summarized in **Supplementary Table 4**.

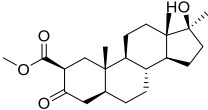
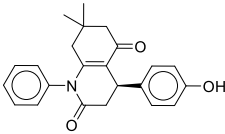
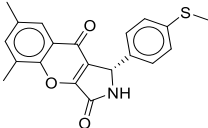
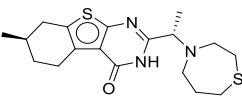
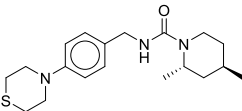
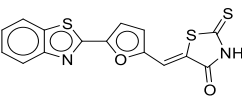
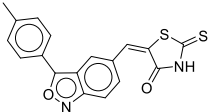
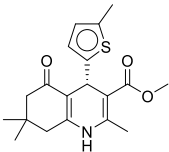
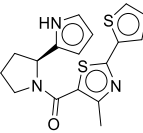
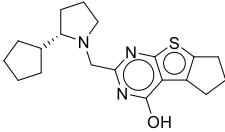
**Supplementary table 4.** Properties of mavoglurant and benchmarking decoys

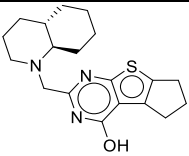
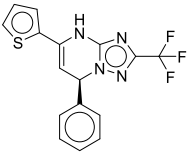
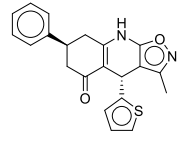
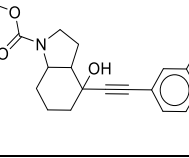
No.	Structures	M.W.	LogP(o/w)	H-bond acceptor	H-bond donor	Number of rotatable bonds
<b>C94605550</b>		349.26	2.61	2	1	2
<b>C94603839</b>		349.26	2.23	2	1	3
<b>C50892585</b>		346.18	3.94	2	1	2
<b>C40285632</b>		346.18	3.86	2	1	2
<b>C89233694</b>		351.27	3.20	3	2	3
<b>C94730376</b>		361.04	3.70	3	1	2
<b>C49773000</b>		348.17	2.69	2	1	3

<b>C54346841</b>		348.17	2.69	2	1	3
<b>C94672645</b>		345.62	2.99	2	1	3
<b>C86415567</b>		353.26	3.73	2	1	3
<b>C18041725</b>		346.23	3.98	4	1	3
<b>C01435425</b>		368.61	4.28	4	1	2
<b>C37968541</b>		351.24	3.70	4	1	4
<b>C91880141</b>		352.23	3.54	4	1	4
<b>C85807545</b>		353.26	3.05	2	1	3
<b>C57549951</b>		350.24	3.35	3	1	3
<b>C85404698</b>		351.24	4.27	0	0	3
<b>C02957825</b>		375.25	4.14	3	1	2

<b>C20560551</b>		347.28	3.12	0	0	3
<b>C88086088</b>		351.24	2.97	2	1	3
<b>C03610264</b>		351.24	3.96	2	1	2
<b>C86379333</b>		353.26	3.27	2	1	3
<b>C96842812</b>		371.30	2.66	2	1	2
<b>C37304332</b>		351.27	3.01	2	1	3
<b>C22319230</b>		352.89	3.52	2	1	4
<b>C52306345</b>		353.85	4.17	3	1	3
<b>C33316201</b>		345.81	4.78	3	1	3
<b>C00287599</b>		344.80	5.75	4	2	3

<b>C02385249</b>		367.37	3.12	3	1	2
<b>C19332894</b>		345.46	4.30	3	1	2
<b>C77543852</b>		347.48	3.65	2	1	5
<b>C90748008</b>		359.21	3.26	2	1	2
<b>C97630911</b>		381.22	3.24	2	1	2
<b>C97605644</b>		375.17	3.95	1	0	2
<b>C03843779</b>		364.53	4.44	4	1	2
<b>C66132068</b>		350.46	4.22	2	1	3
<b>C14480323</b>		374.48	3.33	2	1	3

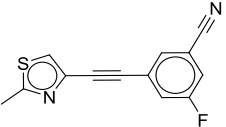
<b>C38331020</b>		362.51	3.69	3	1	2
<b>C00759147</b>		361.44	3.75	3	1	2
<b>C38703321</b>		351.43	3.53	2	1	2
<b>C89982910</b>		363.55	2.92	3	1	2
<b>C77549341</b>		347.53	3.08	1	1	5
<b>C02439112</b>		344.44	3.22	3	1	2
<b>C39895682</b>		352.44	4.30	3	1	2
<b>C00296654</b>		345.46	3.03	2	1	3
<b>C48276740</b>		343.48	2.85	2	1	4
<b>C55927954</b>		343.50	3.97	1	0	3

<b>C67132597</b>		343.50	3.97	1	0	2
<b>C12601193</b>		348.35	3.47	2	1	3
<b>C20715199</b>		362.45	3.37	2	1	2
<b>nam</b>		313.40	3.86	2	1	4

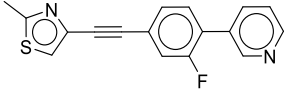
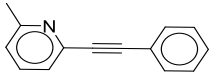
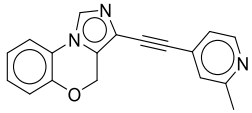
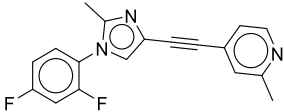
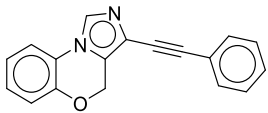
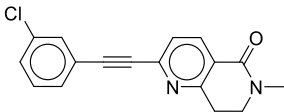
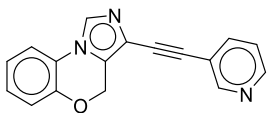
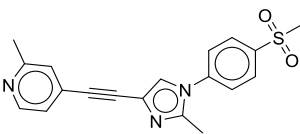
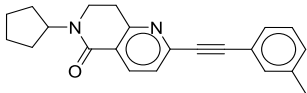
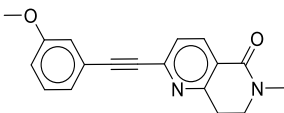
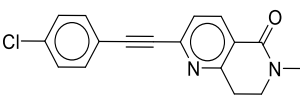
## 7.5 *K<sub>i</sub>* VALUE AND PHYSICAL PROPERTIES OF 66 1,2-DIPHENYLETHYNE ANALOGS

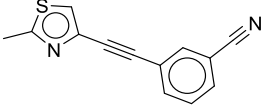
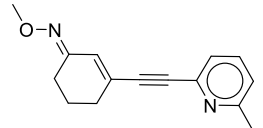
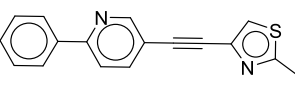
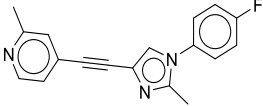
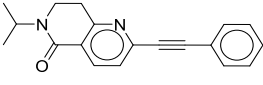
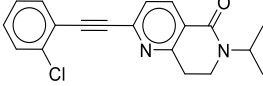
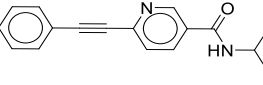
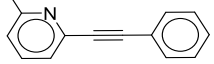
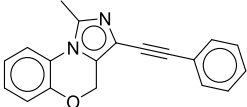
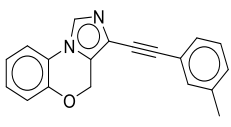
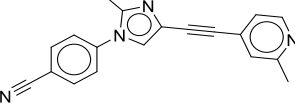
Structure, *K<sub>i</sub>* value, molecular weight, logP (o/w), number of hydrogen bond acceptors, and number of hydrogen bond donors of 66 1,2-diphenylethyne analogs are summarized in **Supplementary Table 5**.

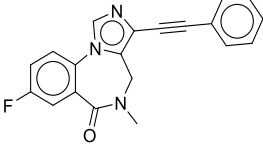
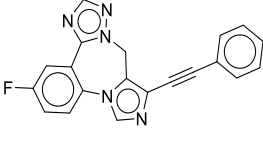
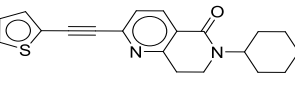
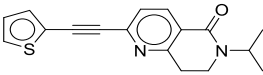
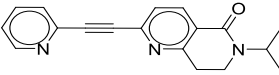
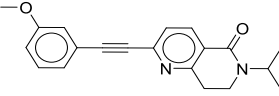
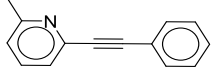
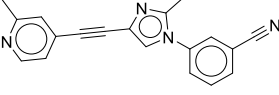
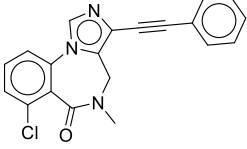
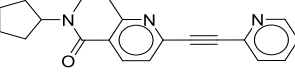
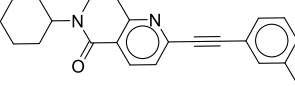
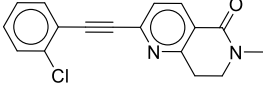
**Supplementary table 5.** *K<sub>i</sub>* value and physical properties of 66 1,2-diphenylethyne analogs

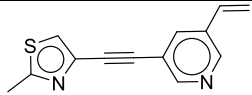
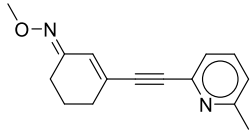
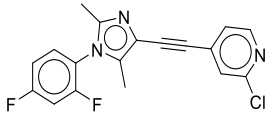
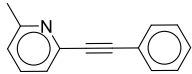
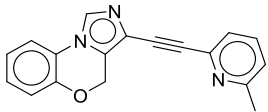
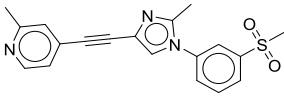
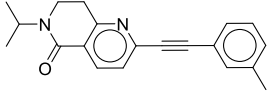
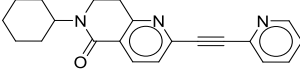
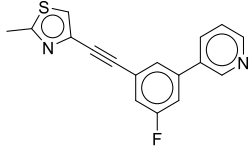
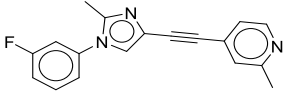
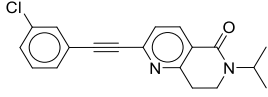
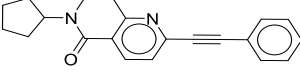
No.	Structures	<i>K<sub>i</sub></i> (nM)	M.W.	LogP (o/w)	H-bond acceptor	H-bond Donor
<b>T1</b>		0.90	242.28	3.44	2	0

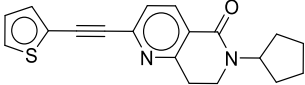
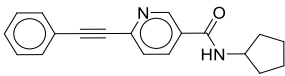
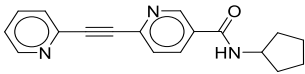
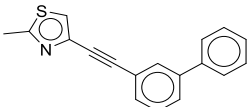
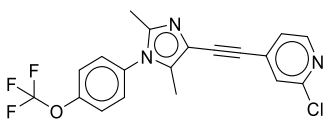
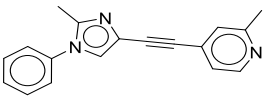
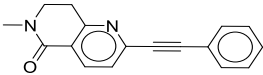
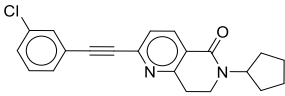
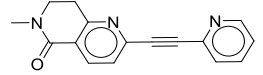
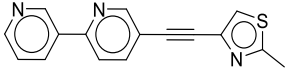
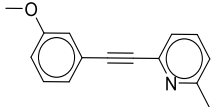
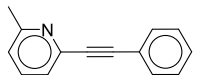
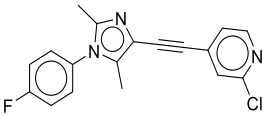


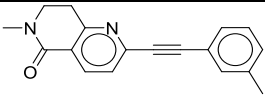
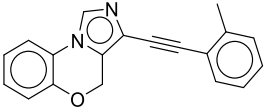
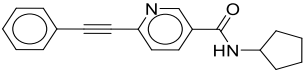
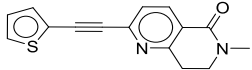
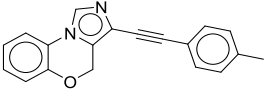
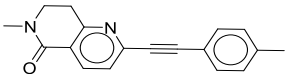
<b>T2</b>		11.40	294.35	4.43	2	0
<b>T3</b>		13.00	193.25	3.77	1	0
<b>T4</b>		18.00	287.32	3.15	3	0
<b>T5</b>		32.00	309.32	4.09	2	0
<b>T6</b>		69.00	272.31	4.09	2	0
<b>T7</b>		250.00	296.76	3.33	2	0
<b>T8</b>		255.00	273.29	2.85	3	0
<b>T9</b>		567.00	351.43	2.95	4	0
<b>T10</b>		670.00	330.43	4.58	2	0
<b>T11</b>		3660.00	292.34	2.70	3	0
<b>T12</b>		6150.00	296.76	3.30	2	0

<b>T13</b>		0.37	224.29	3.21	2	0
<b>T14</b>		3.50	240.31	2.88	2	0
<b>T15</b>		5.49	276.36	4.21	2	0
<b>T16</b>		22.00	291.33	3.90	2	0
<b>T17</b>		1280.00	290.37	3.51	2	0
<b>T18</b>		5680.00	324.81	4.10	2	0
<b>T19</b>		7100.00	264.33	3.44	2	0
<b>T20</b>		3.40	193.25	3.77	1	0
<b>T21</b>		29.00	286.33	4.42	2	0
<b>T22</b>		72.00	286.33	4.42	2	0
<b>T23</b>		83.00	298.35	3.41	3	0

<b>T24</b>		368.00	331.35	3.82	2	0
<b>T25</b>		559.00	341.35	3.38	3	0
<b>T26</b>		720.00	336.46	4.21	2	0
<b>T27</b>		1930.00	296.39	3.04	2	0
<b>T28</b>		2740.00	291.35	2.24	3	0
<b>T29</b>		2950.00	320.39	3.50	3	0
<b>T30</b>		20.00	193.25	3.77	1	0
<b>T31</b>		90.00	298.35	3.44	3	0
<b>T32</b>		1440.00	347.80	4.22	2	0
<b>T33</b>		1770.00	317.39	2.97	3	0
<b>T34</b>		3210.00	344.46	5.02	2	0
<b>T35</b>		7900.00	296.76	3.29	2	0

<b>T36</b>		1.00	226.30	3.16	2	0
<b>T37</b>		1.70	240.31	2.88	2	0
<b>T38</b>		33.00	343.76	5.09	2	0
<b>T39</b>		36.31	193.25	3.77	1	0
<b>T40</b>		213.00	287.32	3.07	3	0
<b>T41</b>		252.00	351.43	2.98	4	0
<b>T42</b>		510.00	304.39	3.84	2	0
<b>T43</b>		2240.00	331.42	3.41	3	0
<b>T44</b>		2.70	294.35	4.51	2	0
<b>T45</b>		17.00	291.33	3.94	2	0
<b>T46</b>		100.00	324.81	4.14	2	0
<b>T47</b>		890.00	316.40	4.24	2	0

<b>T48</b>		2840.00	322.43	3.77	2	0
<b>T49</b>		3300.00	290.37	4.18	2	0
<b>T50</b>		7600.00	291.35	2.91	3	0
<b>T51</b>		10.76	275.38	5.51	1	0
<b>T52</b>		20.00	391.78	6.14	3	0
<b>T53</b>		28.00	273.34	3.75	2	0
<b>T54</b>		760.00	262.31	2.70	2	0
<b>T55</b>		5230.00	350.85	4.87	2	0
<b>T56</b>		6240.00	263.30	1.43	3	0
<b>T57</b>		5.65	277.35	2.97	3	0
<b>T58</b>		10.00	223.27	3.59	2	0
<b>T59</b>		36.00	193.25	3.77	1	0
<b>T60</b>		36.00	325.77	4.90	2	0

<b>T61</b>		820.00	276.34	3.04	2	0
<b>T62</b>		1770.00	286.33	4.38	2	0
<b>T63</b>		1800.00	290.37	4.18	2	0
<b>T64</b>		2170.00	268.34	2.23	2	0
<b>T65</b>		2840.00	286.33	4.38	2	0
<b>T66</b>		7450.00	276.34	3.00	2	0

## 7.6 ABBREVIATIONS

ALDR	Aldose reductase
ASD	Allosteric Database
CCR5	C-C chemokine receptor type 5
CD1A	T-cell surface glycoprotein CD1a
CNS	Central nervous system
CYP	Cytochrome P450
DUD	Directory of useful decoys
DUD-E	Directory of useful decoys, enhanced
ECFP	Extended Connectivity Fingerprint
FBDD	Fragment-based drug discovery

FDA	Food and drug administration
GABA	<i>Gamma</i> -Aminobutyric acid
GDP	Guanosine diphosphate
GPCR	G protein-coupled receptors
GTP	Guanosine-5'-triphosphate
HIV	Human immunodeficiency virus
HTS	High throughput screen
LGA	Lamarckian genetic algorithm
M1AChR	Muscarinic acetylcholine receptor M1
mGlu <sub>5</sub>	Metabotropic glutamate receptor 5
MACCS	Molecular ACCess System
NAM	Negative allosteric modulator
NMR	Nuclear magnetic resonance
OXDA	D-amino-acid oxidase
PAINS	Pan Assay Interference Compounds
PAM	Positive allosteric modulator
PDB	Protein data bank
PLS	Partial least squares
QSAR	Quantitative structure–activity relationship
RECAP	Retrosynthetic combinatorial analysis procedure
RMSD	Root-mean-square deviation
SAM	Silent allosteric modulator
TM	Trans membrane

## 8.0 BIBLIOGRAPHY

1. Wu H, Wang C, Gregory KJ, Han GW, Cho HP, Xia Y, et al. Structure of a class C GPCR metabotropic glutamate receptor 1 bound to an allosteric modulator. *Science*. 2014;344(6179):58-64.
2. Venter JC, Adams MD, Myers EW, Li PW, Mural RJ, Sutton GG, et al. The sequence of the human genome. *science*. 2001;291(5507):1304-51.
3. Overington JP, Al-Lazikani B, Hopkins AL. How many drug targets are there? *Nature reviews Drug discovery*. 2006;5(12):993-6.
4. Feng Z, Hu G, Ma S, Xie X-Q. Computational Advances for the Development of Allosteric Modulators and Bitopic Ligands in G Protein-Coupled Receptors. *The AAPS journal*. 2015;17(5):1080-95.
5. Wenthur CJ, Gentry PR, Mathews TP, Lindsley CW. Drugs for allosteric sites on receptors. *Annual review of pharmacology and toxicology*. 2014;54:165.
6. Wellendorph P, Bräuner-Osborne H. Molecular basis for amino acid sensing by family CG-protein-coupled receptors. *British journal of pharmacology*. 2009;156(6):869-84.
7. Lane JR, Abdul-Ridha A, Canals M. Regulation of G protein-coupled receptors by allosteric ligands. *ACS chemical neuroscience*. 2013;4(4):527-34.
8. Melancon BJ, Hopkins CR, Wood MR, Emmitte KA, Niswender CM, Christopoulos A, et al. Allosteric modulation of seven transmembrane spanning receptors: theory, practice, and opportunities for central nervous system drug discovery. *Journal of medicinal chemistry*. 2012;55(4):1445-64.



9. Christopoulos A. Allosteric binding sites on cell-surface receptors: novel targets for drug discovery. *Nature Reviews Drug Discovery*. 2002;1(3):198-210.
10. Conn PJ, Christopoulos A, Lindsley CW. Allosteric modulators of GPCRs: a novel approach for the treatment of CNS disorders. *Nature reviews Drug discovery*. 2009;8(1):41-54.
11. Bridges TM, Lindsley CW. G-protein-coupled receptors: from classical modes of modulation to allosteric mechanisms. *ACS chemical biology*. 2008;3(9):530-41.
12. Digby GJ, Conn PJ, Lindsley CW. Orthosteric-and allosteric-induced ligand-directed trafficking at GPCRs. *Current opinion in drug discovery & development*. 2010;13(5):587.
13. Fang Z, Grütter C, Rauh D. Strategies for the selective regulation of kinases with allosteric modulators: exploiting exclusive structural features. *ACS chemical biology*. 2012;8(1):58-70.
14. Möhler H, Fritschy J, Rudolph U. A new benzodiazepine pharmacology. *Journal of Pharmacology and Experimental Therapeutics*. 2002;300(1):2-8.
15. Pin J-P, Galvez T, Prézeau L. Evolution, structure, and activation mechanism of family 3/C G-protein-coupled receptors. *Pharmacology & therapeutics*. 2003;98(3):325-54.
16. Doré AS, Okrasa K, Patel JC, Serrano-Vega M, Bennett K, Cooke RM, et al. Structure of class C GPCR metabotropic glutamate receptor 5 transmembrane domain. *Nature*. 2014;511(7511):557-62.
17. Li G, Jørgensen M, Campbell BM. Metabotropic glutamate receptor 5-negative allosteric modulators for the treatment of psychiatric and neurological disorders (2009-July 2013). *Pharmaceutical patent analyst*. 2013;2(6):767-802.

18. Levenga J, Hayashi S, de Vrij FM, Koekkoek SK, van der Linde HC, Nieuwenhuizen I, et al. AFQ056, a new mGluR5 antagonist for treatment of fragile X syndrome. *Neurobiology of disease*. 2011;42(3):311-7.
19. Ritzén A, Sindet R, Hentzer M, Svendsen N, Brodbeck RM, Bundgaard C. Discovery of a potent and brain penetrant mGluR5 positive allosteric modulator. *Bioorganic & medicinal chemistry letters*. 2009;19(12):3275-8.
20. Hajduk PJ, Greer J. A decade of fragment-based drug design: strategic advances and lessons learned. *Nature reviews Drug discovery*. 2007;6(3):211-9.
21. Joseph-McCarthy D, Campbell AJ, Kern G, Moustakas D. Fragment-based lead discovery and design. *Journal of chemical information and modeling*. 2014;54(3):693-704.
22. Allen KN, Bellamacina CR, Ding X, Jeffery CJ, Mattos C, Petsko GA, et al. An experimental approach to mapping the binding surfaces of crystalline proteins. *The Journal of Physical Chemistry*. 1996;100(7):2605-11.
23. Chessari G, Woodhead AJ. From fragment to clinical candidate—a historical perspective. *Drug discovery today*. 2009;14(13):668-75.
24. de Kloe GE, Bailey D, Leurs R, de Esch IJ. Transforming fragments into candidates: small becomes big in medicinal chemistry. *Drug discovery today*. 2009;14(13):630-46.
25. Jencks WP. On the attribution and additivity of binding energies. *Proceedings of the National Academy of Sciences*. 1981;78(7):4046-50.
26. Schneider G, Fechner U. Computer-based de novo design of drug-like molecules. *Nature Reviews Drug Discovery*. 2005;4(8):649-63.

27. Howard N, Abell C, Blakemore W, Chessari G, Congreve M, Howard S, et al. Application of fragment screening and fragment linking to the discovery of novel thrombin inhibitors. *Journal of medicinal chemistry*. 2006;49(4):1346-55.
28. Edwards PD, Albert JS, Sylvester M, Aharony D, Andisik D, Callaghan O, et al. Application of Fragment-Based Lead Generation to the Discovery of Novel, Cyclic Amidine  $\beta$ -Secretase Inhibitors with Nanomolar Potency, Cellular Activity, and High Ligand Efficiency §. *Journal of medicinal chemistry*. 2007;50(24):5912-25.
29. Sun C, Petros AM, Hajduk PJ. Fragment-based lead discovery: challenges and opportunities. *Journal of computer-aided molecular design*. 2011;25(7):607-10.
30. Loving K, Alberts I, Sherman W. Computational approaches for fragment-based and de novo design. *Current topics in medicinal chemistry*. 2010;10(1):14-32.
31. Schuffenhauer A, Ruedisser S, Marzinzik A, Jahnke W, Selzer P, Jacoby E. Library design for fragment based screening. *Current topics in medicinal chemistry*. 2005;5(8):751-62.
32. Siegal G, Eiso A, Schultz J. Integration of fragment screening and library design. *Drug discovery today*. 2007;12(23):1032-9.
33. Lepre C. Fragment-based drug discovery using the SHAPES method. *Expert opinion on drug discovery*. 2007;2(12):1555-66.
34. Fjellström O, Akkaya S, Beisel H-G, Eriksson P-O, Erixon K, Gustafsson D, et al. Creating novel activated factor xi inhibitors through fragment based lead generation and structure aided drug design. *PloS one*. 2015;10(1):e0113705.
35. Ni S, Yuan Y, Huang J, Mao X, Lv M, Zhu J, et al. Discovering potent small molecule inhibitors of cyclophilin A using de novo drug design approach. *Journal of medicinal chemistry*. 2009;52(17):5295-8.

36. Huang Z, Mou L, Shen Q, Lu S, Li C, Liu X, et al. ASD v2. 0: updated content and novel features focusing on allosteric regulation. *Nucleic acids research*. 2014;42(D1):D510-D6.
37. Christopher JA, Aves SJ, Bennett KA, Doré AS, Errey JC, Jazayeri A, et al. Fragment and structure-based drug discovery for a class C GPCR: discovery of the mGlu5 negative allosteric modulator HTL14242 (3-chloro-5-[6-(5-fluoropyridin-2-yl) pyrimidin-4-yl] benzonitrile). *Journal of medicinal chemistry*. 2015;58(16):6653-64.
38. SYBYL-X 1.3 TI, 1699 South Hanley Rd., St. Louis, MO, 63144, USA. 2010.
39. Feng Z, Ma S, Hu G, Xie X-Q. Allosteric binding site and activation mechanism of class C G-protein coupled receptors: metabotropic glutamate receptor family. *The AAPS journal*. 2015;17(3):737-53.
40. The PyMOL Molecular graphics system vS, LLC.
41. Teague SJ, Davis AM, Leeson PD, Oprea T. The design of leadlike combinatorial libraries. *Angewandte Chemie International Edition*. 1999;38(24):3743-8.
42. Lewell XQ, Judd DB, Watson SP, Hann MM. Recap retrosynthetic combinatorial analysis procedure: a powerful new technique for identifying privileged molecular fragments with useful applications in combinatorial chemistry. *Journal of chemical information and computer sciences*. 1998;38(3):511-22.
43. Fechner U, Schneider G. Flux (1): a virtual synthesis scheme for fragment-based de novo design. *Journal of chemical information and modeling*. 2006;46(2):699-707.
44. Jain AN. Scoring noncovalent protein-ligand interactions: a continuous differentiable function tuned to compute binding affinities. *Journal of computer-aided molecular design*. 1996;10(5):427-40.

45. Weiner SJ, Kollman PA, Nguyen DT, Case DA. An all atom force field for simulations of proteins and nucleic acids. *Journal of Computational Chemistry*. 1986;7(2):230-52.
46. Meng EC, Shoichet BK, Kuntz ID. Automated docking with grid-based energy evaluation. *Journal of computational chemistry*. 1992;13(4):505-24.
47. Sanner MF. Python: a programming language for software integration and development. *J Mol Graph Model*. 1999;17(1):57-61.
48. Morris GM, Goodsell DS, Halliday RS, Huey R, Hart WE, Belew RK, et al. Automated docking using a Lamarckian genetic algorithm and an empirical binding free energy function. *Journal of computational chemistry*. 1998;19(14):1639-62.
49. Huang N, Shoichet BK, Irwin JJ. Benchmarking sets for molecular docking. *Journal of medicinal chemistry*. 2006;49(23):6789-801.
50. Weiss DR, Bortolato A, Tehan B, Mason JS. GPCR-Bench: A Benchmarking Set and Practitioners' Guide for G Protein-Coupled Receptor Docking. *Journal of chemical information and modeling*. 2016;56(4):642-51.
51. Mysinger MM, Carchia M, Irwin JJ, Shoichet BK. Directory of useful decoys, enhanced (DUD-E): better ligands and decoys for better benchmarking. *Journal of medicinal chemistry*. 2012;55(14):6582-94.
52. Ioele G, De Luca M, Oliverio F, Ragno G. Prediction of photosensitivity of 1, 4-dihydropyridine antihypertensives by quantitative structure-property relationship. *Talanta*. 2009;79(5):1418-24.
53. Raska I, Toropov A. Comparison of QSPR models of octanol/water partition coefficient for vitamins and non vitamins. *European journal of medicinal chemistry*. 2006;41(11):1271-8.

54. Hogg R, Tanis E. Nonparametric methods. Probability and Statistical Inference, 4th edn MacMillan Publishing Co, New York, USA. 1993:589-646.
55. Hogg RV, Tanis EA. Solutions Manual, Probability and Statistical Interference: Solutions: Macmillan; 1988.
56. Ertl P. Cheminformatics analysis of organic substituents: identification of the most common substituents, calculation of substituent properties, and automatic identification of drug-like bioisosteric groups. Journal of chemical information and computer sciences. 2003;43(2):374-80.
57. Congreve M, Carr R, Murray C, Jhoti H. A 'rule of three' for fragment-based lead discovery? Drug discovery today. 2003;8(19):876-7.
58. Rees DC, Congreve M, Murray CW, Carr R. Fragment-based lead discovery. Nature Reviews Drug Discovery. 2004;3(8):660-72.
59. Lipinski CA, Lombardo F, Dominy BW, Feeney PJ. Experimental and computational approaches to estimate solubility and permeability in drug discovery and development settings. Advanced drug delivery reviews. 2012;64:4-17.
60. Bogan AA, Thorn KS. Anatomy of hot spots in protein interfaces. Journal of molecular biology. 1998;280(1):1-9.
61. Leffler JE. The enthalpy-entropy relationship and its implications for organic chemistry. The Journal of Organic Chemistry. 1955;20(9):1202-31.
62. Eftink MR, Anusiem A, Biltonen RL. Enthalpy-entropy compensation and heat capacity changes for protein-ligand interactions: general thermodynamic models and data for the binding of nucleotides to ribonuclease A. Biochemistry. 1983;22(16):3884-96.

63. Davenport AP, Russell FD. Radioligand binding assays: theory and practice. *Current Directions in Radiopharmaceutical Research and Development*: Springer; 1996. p. 169-79.
64. Cui W, Yan X. Adaptive weighted least square support vector machine regression integrated with outlier detection and its application in QSAR. *Chemometrics and Intelligent Laboratory Systems*. 2009;98(2):130-5.
65. Baell JB, Holloway GA. New substructure filters for removal of pan assay interference compounds (PAINS) from screening libraries and for their exclusion in bioassays. *Journal of medicinal chemistry*. 2010;53(7):2719-40.
66. Patlewicz G, Jeliaskova N, Safford R, Worth A, Aleksiev B. An evaluation of the implementation of the Cramer classification scheme in the Toxtree software. *SAR and QSAR in Environmental Research*. 2008;19(5-6):495-524.
67. Bursavich MG, Gilbert AM, Stock JR. Piperazine Metabotropic Glutamate Receptor 5 (MGLUR5) Negative Allosteric Modulators For Anxiety/Depression. US Patents; 2009.
68. Macdonald G, Tresadern G, Trabanco-Suarez A, Pastor-Fernandez J. Preparation of Bicyclic Thiazoles as Allosteric Modulators of mGluR5 Receptors. WO Patent 2011073339A1; 2011.
69. Imogai H, Mutel V, Duvey GA, Cid-Nunez J, Le Poul E, Lutjens R. Novel thienopyridine and thieno-pyrimidine derivatives and their use as positive allosteric modulators of mGluR2-receptors. Google Patents; 2005.
70. Conn J, Lindsley C, Weaver C, Stauffer S, Williams R, McDonald G, et al. Preparation of O-benzyl nicotinamide analogs as mGluR5 positive allosteric modulators. WO2011035324. 2011.

71. Imogai HJ, Cid-Nunez JM, Andres-Gil JI, Trabanco-Suarez AA, Santamarina JO, Dautzenberg FM, et al. 1, 4-Disubstituted 3-Cyano-Pyridone Derivatives and Their Use As Positive Allosteric Modulators of MGLUR2-Receptors. Google Patents; 2014.